

TMUP-HEL-9704

FTUV/97-21

IFIC/97-21

hep-ph/9705208

Revised December 1997

CP Violation vs. Matter Effect in Long-Baseline Neutrino Oscillation Experiments

Hisakazu Minakata¹ and Hiroshi Nunokawa²

¹*Department of Physics, Tokyo Metropolitan University*

Minami-Osawa, Hachioji, Tokyo 192-03, Japan

²*Instituto de Física Corpuscular - C.S.I.C.*

Department of Física Teòrica, Universitat de València,

46100 Burjassot, Valencia, Spain

(April, 1997)

Abstract

We investigate, within the framework of three generations of neutrinos, the effects of CP violation in long-baseline neutrino oscillation experiments. We aim at illuminating the global feature of the interplay between genuine effect due to the CP violating phase and a fake one due to the earth matter effect. To this goal, we develop a formalism based on the adiabatic approximation and perturbative treatment of the matter effect which allows us to obtain approximate analytic expressions of the oscillation probabilities. We present

an order-of-magnitude estimation and a detailed numerical computation of the absolute and the relative magnitudes of the CP violations under the mass hierarchy suggested by the atmospheric neutrino anomaly and the cosmological dark matter. We find that the genuine CP violating effect is at most $\sim 1\%$, and the matter effect dominates over the intrinsic CP violation only in a region of parameters where the oscillation probability of $\nu_\mu \rightarrow \nu_e$ is large.

14.60.Pq, 25.30.Pt, 95.35.+d

I. INTRODUCTION

The origin of CP violation is still a mystery in particle physics. Unlike in the quark sector even the very existence of CP violation is not known in the lepton sector. Recent advances in neutrino observations mainly of astrophysical origins strongly suggest the existence of tiny neutrino masses [1,2]. If this is the case nature would admit the Cabibbo-Kobayashi-Maskawa (CKM) [3] type flavor mixing also in the lepton sector which allows us to have CP violating phases with three (or more) generation of leptons. If revealed, it should give us important insight into our understanding of fundamental structure of matter. Moreover, there is an intriguing suggestion [4] that CP violation in the lepton sector might be an indispensable ingredient in producing the baryon asymmetry in the universe.

It has been known since long time ago [5] that the effect of CP violating phase can in principle be observable in neutrino oscillation experiments. The other earlier references include [6–8]. As we will recapitulate below the particle-antiparticle difference between the oscillation probabilities, $\Delta P(\nu_\beta \rightarrow \nu_\alpha) \equiv P(\nu_\beta \rightarrow \nu_\alpha) - P(\bar{\nu}_\beta \rightarrow \bar{\nu}_\alpha)$, in vacuum is characterized [6,7] by the leptonic analogue of the Jarlskog factor, the unique and phase-convention independent measure for CP violation [9].

Recently, measuring leptonic CP violation in the long-baseline neutrino oscillation experiments [10–12] received considerable amount of attention in the literature [13,14]. The potential obstacle in measuring CP violation in the long-baseline experiment is the matter effect in the earth. It is well known that the matter effect acts differently in propagation of ν and $\bar{\nu}$ in matter; it gives rise to the index of refraction which differs in sign between ν and $\bar{\nu}$ [15]. Then, the $\nu - \bar{\nu}$ difference ΔP of the oscillation probabilities is inevitably contaminated by the matter effect [16]. In fact, it is known by numerical computation that the matter effect is overwhelming over the genuine CP violating effect at certain values of the mixing parameters in the $\nu_\mu \rightarrow \nu_e$ channel [13,14]. But it appears to the authors that we still lack understanding of the over-all features of the relationship between the CP violations due to the matter and to the CP violating phases.

It is the purpose of the present paper to illuminate global structure of the interplay between the matter and the genuine CP violating effects in long-baseline experiments. To this goal we develop a formalism by which we can derive approximate analytic expressions of oscillation probabilities. These analytic formulas will allow us to have global view of the features of CP violation in neutrino oscillation experiments. Our formalism is based on the adiabatic approximation and takes into account the matter effect in a perturbative way. It also enjoys further simplification due to the presumed hierarchy of neutrino masses which will be explained below.

This is the first in a series of papers to investigate the same problem in various neutrino mass hierarchies. In this paper, we assume that the atmospheric neutrino anomaly, which is observed by the Kamiokande, IMB, and the Soudan 2 experiments [2], can be interpreted as the evidence for neutrino oscillations whose relevant mass scale is $\Delta m^2 \sim 10^{-2} \text{ eV}^2$ or larger. (We note, however, that the two experiments do not observe the atmospheric neutrino anomaly [17].) It is a natural assumption because it is the very motivation for planning the long-baseline experiments. The restriction leads to the hierarchy between the matter potential and the mass differences, which allows us to treat the matter effect perturbatively. Namely, we derive closed-form analytic expressions of the neutrino-antineutrino difference between oscillation probabilities which is generally valid under the adiabatic approximation and a first-order perturbative treatment of the matter effect.

We restrict ourselves into the case of neutrino mass hierarchy motivated by the cosmological hot dark matter [18] in our analysis of the features of CP violation in this paper. The assumption of the dark matter scale mass difference allows us to utilize the strong constraints on the mixing parameters deduced from the terrestrial experiments [19]. It is the reason why we decided to investigate this case first; Because of the constraints we are able to estimate the magnitude of CP violation in a less ambiguous way.

We give a few word on the problem if the mass hierarchy we examine in this paper can account for the other known hints for the neutrino masses. They include the solar neutrino deficit [1] and the LSND experiments [20]. Let us first discuss the solar neutrinos. It is well

known that for this scheme the capability of explaining the gross deficit of the solar neutrino flux depends upon the parameter regions. In the region (A) (see Eq. (10) for the definitions of these regions) the global deficit of the flux can be accommodated in a manner of Acker and Pakvasa [21]. In the region (B) there is no way of having a gross deficit of the solar neutrino flux within the framework of three-flavor mixing. Therefore, we must introduce some other ingredients such as sterile neutrinos to achieve the deficit in the region (B).

The results of the LSND experiments can be easily accommodated in the present framework. The LSND data allow the mass scales which is consistent with hot dark matter. If smaller values of Δm^2 is preferred for consistency with other experiments it may be necessary to relax the constraints on the mass scale required by the mixed dark matter cosmology [18]. If the simultaneous consistency with the solar neutrino and the LSND data is demanded there is no solution within our present framework.

Within the restrictions to the mass hierarchies hinted by the dark matter and the atmospheric neutrinos, we will try to answer the following questions:

- (1) Are there any channels which are much less contaminated by the matter effect?
- (2) In which parameter regions do we expect to have maximal CP violation and how large is its size?

It is known that the matter effect in the oscillation probability in long-baseline experiments is not very large, at most a few to several %. One might then feel strange that the matter effect is dominant in certain channel. The point is that what we are dealing with is not the oscillation probability itself but the difference between the neutrino and the antineutrino oscillation probabilities. The matter effect can give rise to a dominant effect in such $\nu - \bar{\nu}$ difference.

This investigation was motivated by a question asked by a long-baseline neutrino experimentalist [22]; “Is the matter effect contamination small in $\nu_\mu \rightarrow \nu_\tau$ channel?” This is the interesting question for two reasons, one theoretical and one experimental. Experimentally it is a very relevant question because they are planning to do long-baseline neutrino experiments in the appearance channel, $\nu_\mu \rightarrow \nu_\tau$. It is also of interest from the theoretical

point of view; In the conventional treatment of “optional” two-flavor mixing favored by experimentalists the $\nu_\mu \rightarrow \nu_\tau$ channel might be free from the matter effect because there is no μ ’s and τ ’s in the earth. On the other hand, CP violation is the genuine three-flavor mixing effect which cannot occur in two-flavor mixing framework. Therefore, the question still remains whether the matter effect is small in the $\nu_\mu \rightarrow \nu_\tau$ channel, as correctly raised by the experimentalist.

In Sec. II, we review some basic facts on CP violation in vacuum in the context of neutrino oscillation experiments. We also summarize the mass patterns of neutrinos which we use in our analysis in this paper. In Sec. III, we set up our formalism based on the adiabatic approximation. In Sec. IV, we develop a framework for perturbative treatment of the matter effect which is applicable to the long-baseline neutrino experiments. In Sec. V, we derive the approximate analytic formulas for the neutrino-antineutrino difference in oscillation probabilities by taking account of the matter effect to first-order in perturbation theory. In Sec. VI, we use our analytic formula to illuminate global features of the competing two effects producing CP violation, the genuine effect due to CP violating phase and a fake one due to the matter effect. In Sec. VII, we give the results of our detailed numerical computation of the CP violation to confirm the qualitative understanding of the structure of the coexisting two effects obtained in Sec. VI. The last section VIII is devoted to the conclusion. In Appendix we confirm that the adiabatic approximation is in fact a very good approximation for matter density profiles relevant for the long-baseline experiments.

II. CP VIOLATION IN VACUUM AND NEUTRINO MASS SPECTRUM MOTIVATED BY DARK MATTER AND ATMOSPHERIC NEUTRINO ANOMALY

In this section we first review briefly the CP violation in neutrino oscillations in vacuum. We then describe the neutrino mass spectrum which we consider in this paper. It is intended for convenience for the readers who are not familiar to the subject and precedes the following

three sections in which we develop our analytic framework usable for analyses with more general neutrino mass patterns.

We work with the three-flavor mixing scheme of neutrinos and introduce the flavor mixing matrix U as

$$\nu_\alpha = U_{\alpha i} \nu_i, \quad (1)$$

where $\nu_\alpha (\alpha = e, \mu, \tau)$ and $\nu_i (i = 1, 2, 3)$ stand for the gauge and the mass eigenstates, respectively. Then in vacuum the direct measure of CP violation can be written [6,7] as

$$\Delta P(\nu_\beta \rightarrow \nu_\alpha) \equiv P(\nu_\beta \rightarrow \nu_\alpha) - P(\bar{\nu}_\beta \rightarrow \bar{\nu}_\alpha) = -4J_{\beta\alpha}(\sin \Delta_{12} + \sin \Delta_{23} + \sin \Delta_{31}), \quad (2)$$

where

$$\Delta_{ij} \equiv \frac{(m_j^2 - m_i^2)L}{2E}, \quad (3)$$

with $m_i (i = 1, 2, 3)$ being the mass of i -th neutrino, E the neutrino energy and L the distance from the neutrino source. We have used in (2) the Jarlskog parameter

$$J_{\beta\alpha} \equiv \text{Im}[U_{\alpha 1} U_{\alpha 2}^* U_{\beta 1}^* U_{\beta 2}] \quad (4)$$

which is unique, up to the sign, in three-flavor neutrinos.

We will use the following form of the neutrino mixing matrix

$$U = \begin{bmatrix} c_{12}c_{13} & s_{12}c_{13} & s_{13}e^{-i\delta} \\ -s_{12}c_{23} - c_{12}s_{23}s_{13}e^{i\delta} & c_{12}c_{23} - s_{12}s_{23}s_{13}e^{i\delta} & s_{23}c_{13} \\ s_{12}s_{23} - c_{12}c_{23}s_{13}e^{i\delta} & -c_{12}s_{23} - s_{12}c_{23}s_{13}e^{i\delta} & c_{23}c_{13} \end{bmatrix}, \quad (5)$$

which is identical with the standard CKM matrix for quarks. Here $c_{ij} \equiv \cos \theta_{ij}$ and $s_{ij} \equiv \sin \theta_{ij}$ where $(i, j) = (1, 2), (2, 3)$ and $(1, 3)$. With this parametrization $J_{\beta\alpha}$ can be expressed as

$$J_{\beta\alpha} = \pm J, \quad J \equiv c_{12}s_{12}c_{23}s_{23}c_{13}^2s_{13} \sin \delta, \quad (6)$$

where $+$ sign is for cyclic permutations, i.e., $(\alpha, \beta) = (e, \mu), (\mu, \tau), (\tau, e)$ and $-$ is for anti-cyclic ones.

Let us come to the mass hierarchy which will be used in our analysis presented in Secs. VI and VII. We work with the mass hierarchy

$$|\Delta m^2| \sim 10^{-2} \text{eV}^2, \quad \Delta m^2 \equiv m_2^2 - m_1^2, \quad (7)$$

$$|\Delta M^2| \gtrsim \text{a few eV}^2, \quad \Delta M^2 \equiv m_3^2 - m_1^2 \simeq m_3^2 - m_2^2, \quad (8)$$

where the first is suggested by the atmospheric neutrino anomaly [2], and the second is motivated by the hot and the cold dark matter cosmology [18].

The Kamiokande, IMB, and the Soudan 2 experiments observed a 30-40 % deficit in the double ratio $(\frac{\nu_\mu}{\nu_e})_{\text{observed}}/(\frac{\nu_\mu}{\nu_e})_{\text{expected}}$ [2]. A natural interpretation of the anomaly is due to the neutrino oscillation. In particular, the multi-GeV data from the Kamiokande experiments indicates that the double ratio has a zenith-angle dependence which is quite consistent with the interpretation of the anomaly as the evidence for neutrino oscillations with the mass difference $\Delta m^2 \sim 10^{-2} \text{eV}^2$.

The hot and the cold dark matter cosmology is one of the viable models of the structure formation in the universe [18]. The hot dark matter is the indispensable ingredient in the scenario by which the magnitude of density fluctuation normalized by COBE data can be made consistent with that of small scales determined by correlations between galaxies and clusters [23]. Neutrinos of masses 2-20 eV are the natural candidate for the hot dark matter. In fact, it is the only known particles among the candidates for particle dark matter.

The advantage of the dark matter motivated mass hierarchy (8) is that the mixing parameters are subject to the powerful constraints that comes from the reactor and the accelerator experiments [19] and we can draw a clear answer to the question on how large is the magnitude of CP violation.

Under the assumption (8) the oscillations due to the larger mass squared difference ΔM^2 are averaged out in long-baseline experiments and we have,

$$\Delta P(\nu_\beta \rightarrow \nu_\alpha) \sim -4J_{\alpha\beta} \sin\left(\frac{\Delta m^2 L}{2E}\right) \quad (9)$$

Since $\left(\frac{\Delta m^2 L}{2E}\right) = 2.5 \left(\frac{\Delta m^2}{10^{-2} \text{eV}^2}\right) \left(\frac{L}{100 \text{km}}\right) \left(\frac{E}{1 \text{GeV}}\right)^{-1}$ can be of order unity in long-baseline

experiments, the CP violation $\Delta P_{\beta\alpha}$ can be approximated as $\sim -4J_{\alpha\beta}$.

Let us estimate how large CP violation can be for our choice of mass hierarchy (7) and (8). In Fig. 1 we present equal- J contours on $\tan^2 \theta_{13} - \tan^2 \theta_{23}$ plane with use of the parameters $\theta_{12} = \pi/4$ and $\delta = \pi/2$ which maximize J . In the same figure we also plot the regions of parameters excluded by the reactor and accelerator experiments for the case $|\Delta M^2| = 5 \text{ eV}^2$ obtained in Ref. [24]. We notice from Fig. 1 that allowed parameters are restricted into three separate regions.

- (A) small $-s_{13}$ and small $-s_{23}$
- (B) large $-s_{13}$ and arbitrary $-s_{23}$ (10)
- (C) small $-s_{13}$ and large $-s_{23}$

The constraints from the reactor and accelerator experiments are so strong that one neutrino flavor almost decouples with the remaining two. Namely, the ν_τ , ν_e and ν_μ almost decouple with the other two flavors in the regions (A), (B) and (C), respectively. The remaining two neutrinos can be strongly mixed with each other in each allowed region. We observe that the value of $4J$ is at most $\simeq 0.01$ in the regions (A) and (B) and $\simeq 0.001$ in the region (C).

In Fig. 2 we show the neutrino mass spectrum which is realized in the region (A) and (B). We do not consider in this paper the region (C) since the atmospheric neutrino anomaly cannot be accounted for and moreover CP violation is very small in this region. There exist two different mass patterns which can be realized in each parameter regions. Depending upon the sign of ΔM^2 the decoupled state ν_3 can be the heaviest, (A-1) or (B-1), or the lightest, (A-2) or (B-2). The case (A-1) is theoretically appealing because of the seesaw mechanism [25] and from the observed mass hierarchy among charged leptons.

III. ADIABATIC NEUTRINO EVOLUTION IN MATTER

We discuss the neutrino propagation in the earth matter within the framework of three-flavor mixing of neutrinos. It is worth to note that when we discuss the long-baseline

experiments whose baseline distances less than 1000 km the adiabatic approximation is a very good approximation, as we demonstrate in Appendix. It is because the neutrino beam only passes through thin layer of the continental structure closest to the earth surface in which the matter density is approximately constant, $\simeq 2.72 \text{ g/cm}^3$ [26]. By virtue of this fact we can derive a general closed form expression of ΔP , the $\nu - \bar{\nu}$ difference in oscillation probabilities.

The evolution equation of neutrinos (and antineutrinos) can be written in terms of the gauge eigenstate as

$$i \frac{d}{dx} \begin{bmatrix} \nu_e \\ \nu_\mu \\ \nu_\tau \end{bmatrix} = H(x) \begin{bmatrix} \nu_e \\ \nu_\mu \\ \nu_\tau \end{bmatrix}, \quad (11)$$

where the Hamiltonian $H(x)$ is given by

$$H = U \begin{bmatrix} m_1^2/2E & 0 & 0 \\ 0 & m_2^2/2E & 0 \\ 0 & 0 & m_3^2/2E \end{bmatrix} U^\dagger + \begin{bmatrix} a(x) & 0 & 0 \\ 0 & 0 & 0 \\ 0 & 0 & 0 \end{bmatrix}, \quad (12)$$

where x is the position along the neutrino trajectory. Here $a(x)$ represents the matter effect and has the form

$$a(x) = \pm \sqrt{2} G_F N_e(x) \quad (13)$$

where G_F is the Fermi constant, $N_e(x)$ is the electron number density at x in the earth, and the $+$ and $-$ signs are for neutrinos and antineutrinos, respectively.

We introduce the unitary transformation $V(x)$ which diagonalize $H(x)$ locally, i.e., at each point x of neutrino trajectory;

$$V^\dagger(x) H(x) V(x) = H_d(x) \quad (14)$$

and parametrize the diagonalized Hamiltonian as $H_d(x) = \text{diag.}[h_1(x), h_2(x), h_3(x)]$. We then define the matter-mass eigenstate, mass eigenstate basis in matter, as

$$\begin{bmatrix} \nu_{m_1} \\ \nu_{m_2} \\ \nu_{m_3} \end{bmatrix} = V^+(x) \begin{bmatrix} \nu_e \\ \nu_\mu \\ \nu_\tau \end{bmatrix}, \quad (15)$$

The neutrino evolution equation in terms of the matter-mass eigenstate takes the form

$$i \frac{d}{dx} \begin{bmatrix} \nu_{m_1} \\ \nu_{m_2} \\ \nu_{m_3} \end{bmatrix} = H_d(x) \begin{bmatrix} \nu_{m_1} \\ \nu_{m_2} \\ \nu_{m_3} \end{bmatrix} + i \frac{d}{dx} V^+(x) \cdot V(x) \begin{bmatrix} \nu_{m_1} \\ \nu_{m_2} \\ \nu_{m_3} \end{bmatrix}. \quad (16)$$

The adiabatic approximation amounts to ignore the second term in the right-hand-side of eq. (16). We will return in Appendix to the question if it gives a really good approximation.

Under the adiabatic approximation it is straightforward to solve the evolution equation as

$$\nu_\alpha(x) = V_{\alpha i}(x) \exp \left\{ -i \int_0^x dx' h_i(x') \right\} V_{\beta i}^*(0) \nu_\beta(0). \quad (17)$$

We then obtain the probability of the neutrino oscillation $\nu_\beta \rightarrow \nu_\alpha$ where ν_β is created at $x = 0$ and ν_α is detected at $x = L$. It reads

$$P(\nu_\beta \rightarrow \nu_\alpha) = \sum_{i,j} V_{\alpha i}(L) V_{\alpha j}^*(L) V_{\beta i}^*(0) V_{\beta j}(0) \times \exp \left\{ -i \int_0^L dx [h_i(x) - h_j(x)] \right\}. \quad (18)$$

We assume in this paper an idealized situation where the matter densities at the production and the detection points are identical. This should give a good approximation to the real experimental situation because these points are either on or are very close to the earth surface. One way argue that one can take $V(0) = V(L)$ equal to the vacuum mixing matrix U by saying that we design the experiment so that the production and the detection points of neutrinos on the earth surface, namely, in vacuum. We argue that even with such experimental condition it is the better approximation to take as $V(0) = V(L)$ the value of matter-mass mixing matrix with matter density $\sim 2.7 \text{ g/cm}^3$ at just below the earth surface. First of all, if we take the vacuum mixing matrix U for $V(0) = V(L)$ we have to

worry about the failure of the adiabaticity condition at the earth surface. The oscillation length of neutrinos is approximately given by

$$L = 2.5 \left(\frac{E}{1\text{GeV}} \right) \left(\frac{\Delta m^2}{1\text{eV}^2} \right)^{-1} \text{ km} \quad (19)$$

and is much longer than the decay tunnel or the detector hole for interesting regions of Δm^2 . Therefore, the neutrinos do not know if they take off at the earth surface prior to the detection and would rather feel as if they remain in the earth matter at the point of detection.

By separating the summation into $i = j$ and $i \neq j$ terms one can rewrite the expression of oscillation probability into the form

$$\begin{aligned} P(\nu_\beta \rightarrow \nu_\alpha ; \delta, a) = & -4 \sum_{j>i} \text{Re}[V_{\alpha i}(a)V_{\alpha j}^*(a)V_{\beta i}^*(a)V_{\beta j}(a)] \sin^2\left[\frac{1}{2}I_{ij}(a)\right] \\ & + 2 \sum_{j>i} \text{Im}[V_{\alpha i}(a)V_{\alpha j}^*(a)V_{\beta i}^*(a)V_{\beta j}(a)] \sin^1[I_{ij}(a)], \end{aligned} \quad (20)$$

where

$$I_{ij}(a) = \int_0^L dx [h_i(x) - h_j(x)]. \quad (21)$$

IV. PERTURBATIVE TREATMENT OF MATTER EFFECT

Now we intend to evaluate ΔP to first-order in matter perturbation theory. Let us first confirm that the perturbative treatment is reliable under the mass scale with which we are working. Since we are assuming the mass difference $\Delta m^2 \sim 10^{-2} \text{ eV}^2$ relevant for atmospheric neutrino anomaly we have,

$$\frac{\Delta m^2}{E} = 10^{-11} \left(\frac{\Delta m^2}{10^{-2}\text{eV}^2} \right) \left(\frac{E}{1\text{GeV}} \right)^{-1} \text{ eV}. \quad (22)$$

On the other hand, we estimate the matter potential for the continental structure as,

$$a = 1.04 \times 10^{-13} \left(\frac{\rho}{2.7\text{g/cm}^3} \right) \left(\frac{Y_e}{0.5} \right) \text{ eV}, \quad (23)$$

where $Y_e \equiv N_p/(N_p + N_n)$ is the electron fraction. Hence we see that the hierarchy between the energy scales, $a \ll \frac{\Delta m^2}{E}$ (atmospheric mass scale), holds.

We use stationary state perturbation theory in accord with the slow variation of $a(x)$ on which the adiabatic approximation is based. It is convenient to take the vacuum mass eigenstate $\nu_i (i = 1, 2, 3)$, which diagonalizes the unperturbed Hamiltonian, as the basis of matter perturbation theory. We denote the first and the second terms of the Hamiltonian (12) as H_0 and H' , respectively. We use the vacuum mass eigenstate ν_i defined by

$$\nu_i(x) = e^{-ih_i^{(0)}x} \nu_i, \quad (24)$$

where $h_i^{(0)} = m_i^2/2E$, as the basis of matter perturbation theory.

The Hamiltonians in this basis are $\tilde{H}_0 = U^+ H_0 U$ and $\tilde{H}' = U^+ H' U$, respectively. Since $(H')_{\alpha\beta} = a\delta_{\alpha e}\delta_{\beta e}$ we have

$$(\tilde{H}')_{ji} = aU_{ei}U_{ej}^* \quad (25)$$

Then, the matter mass eigenstate can be expressed to first order in a as

$$\nu_{mi} = \nu_i + \sum_{j \neq i} \frac{aU_{ei}^*U_{ej}}{h_i^{(0)} - h_j^{(0)}} \nu_j \quad (26)$$

It can be converted to the expression of vacuum mass eigenstate expressed by the matter mass eigenstate

$$\nu_i = \nu_{mi} - \sum_{j \neq i} \frac{aU_{ei}^*U_{ej}}{h_i^{(0)} - h_j^{(0)}} \nu_{mj} \quad (27)$$

Since the flavor eigenstate has the simple relationship with the vacuum mass eigenstate as

$\nu_\alpha = U_{\alpha i} \nu_i$ we obtain

$$\nu_\alpha = \sum_i \left[U_{\alpha i} \delta_{ij} - \sum_{j \neq i} \frac{U_{\alpha i} U_{ei}^* U_{ej}}{h_i^{(0)} - h_j^{(0)}} a \right] \nu_{mj} \quad (28)$$

The matrix element of V can be read off from this equation as

$$V_{\alpha i} = U_{\alpha i} - \sum_{j \neq i} \frac{U_{\alpha j} U_{ej}^* U_{ei}}{h_j^{(0)} - h_i^{(0)}} a \quad (29)$$

It is instructive to verify that $V_{\alpha i}$ in (29) satisfies the unitarity to first order in a , as it should.

We have obtained the matrix V in the form $V = U + \delta V$, where δV denotes the correction first order in a . Then we can write, schematically, $VVVV$ in (20) as

$$VVVV = UUUU + UUU\delta V \quad (30)$$

where the second term actually contains four pieces. It is important to know the symmetry property of these terms. It follows that

$$\begin{aligned} \text{Re}(UUUU) & \xrightarrow{\delta \rightarrow -\delta} \text{Re}(UUU\delta V) \\ \text{Im}(UUUU) & \xrightarrow{\delta \rightarrow -\delta} -\text{Im}(UUUU) \\ \text{Re}(UUU\delta V) & \xrightarrow{\delta \rightarrow -\delta, a \rightarrow -a} -\text{Re}(UUU\delta V) \\ \text{Im}(UUU\delta V) & \xrightarrow{\delta \rightarrow -\delta, a \rightarrow -a} \text{Im}(UUU\delta V). \end{aligned} \quad (31)$$

They stem from the fact that $UUU\delta V$ is linear in a and that the transformation $\delta \rightarrow -\delta$ is equivalent to $U \rightarrow U^*$.

V. CP VIOLATION EFFECT IN THE PRESENCE OF MATTER

The neutrino-antineutrino difference can be written as

$$\begin{aligned} \Delta P(\nu_\beta \rightarrow \nu_\alpha) & \equiv P(\nu_\beta \rightarrow \nu_\alpha) - P(\bar{\nu}_\beta \rightarrow \bar{\nu}_\alpha) \\ & = P(\nu_\beta \rightarrow \nu_\alpha; \delta, a) - P(\nu_\beta \rightarrow \nu_\alpha; -\delta, -a) \end{aligned} \quad (32)$$

Thanks to the symmetry properties (31), we can express eq. (32) as,

$$\begin{aligned} \Delta P(\nu_\beta \rightarrow \nu_\alpha) & = -4 \sum_{j>i} \text{Re}(UUUU)_{\alpha\beta; ij} \left[\sin^2\left\{\frac{1}{2}I_{ij}(a)\right\} - \sin^2\left\{\frac{1}{2}I_{ij}(-a)\right\} \right] \\ & \quad + 2 \sum_{j>i} \text{Im}(UUUU)_{\alpha\beta; ij} \left[\sin I_{ij}(a) + \sin I_{ij}(-a) \right] \\ & \quad - 4 \sum_{j>i} \text{Re}(UUU\delta V)_{\alpha\beta; ij} \left[\sin^2\left\{\frac{1}{2}I_{ij}(a)\right\} + \sin^2\left\{\frac{1}{2}I_{ij}(-a)\right\} \right] \\ & \quad + 2 \sum_{j>i} \text{Im}(UUU\delta V)_{\alpha\beta; ij} \left[\sin I_{ij}(a) - \sin I_{ij}(-a) \right], \end{aligned} \quad (33)$$

where

$$(UUUU)_{\alpha\beta;ij} = U_{\alpha i} U_{\alpha j}^* U_{\beta i}^* U_{\beta j} \quad (34)$$

etc. We note that the last term in (33) is at least second order in a .

The energy eigenvalue h_i can also be obtained to first order in a as

$$h_i = \frac{m_i^2}{2E} + |U_{ei}|^2 a. \quad (35)$$

Therefore, $I_{ij}(a)$ defined in (21) can be given by

$$I_{ij}(a) = -\frac{\Delta m_{ij}^2}{2E} L + (|U_{ei}|^2 - |U_{ej}|^2) \int_0^L dx a(x), \quad (36)$$

where $\Delta m_{ij}^2 \equiv m_j^2 - m_i^2$. Up to this point one discussion relies only on the hierarchy $a \ll |\Delta m_{ij}^2|/E$ and the hierarchy among Δm_{ij}^2 need not to be assumed.

To obtain an explicit form of ΔP we need the expression of $UUU\delta V$. Due to the mass hierarchy (7) and (8), we can combine the terms and calculate $\sum_{i=1,2} (UUU\delta V)_{\alpha,\beta;i3}$ by ignoring the difference between Δm_{13}^2 and Δm_{23}^2 . We also calculate the sum $(UUU\delta V)_{\alpha,\beta;12}$ separately:

$$\sum_{i=1,2} (UUU\delta V)_{\alpha\beta;i3} = \frac{4Ea}{\Delta M^2} |U_{e3}|^2 \left[2|U_{\alpha 3}|^2 |U_{\beta 3}|^2 - (\delta_{\alpha e} |U_{\beta 3}|^2 + \delta_{\beta e} |U_{\alpha 3}|^2) \right] \quad (37)$$

$$\begin{aligned} & (UUU\delta V)_{\alpha\beta;12} \\ &= -\frac{2Ea}{\Delta m^2} \left[U_{e1}^* U_{e2} U_{\alpha 1} U_{\alpha 2}^* (|U_{\beta 2}|^2 - |U_{\beta 1}|^2) + U_{e1} U_{e2}^* U_{\beta 1}^* U_{\beta 2} (|U_{\alpha 2}|^2 - |U_{\alpha 1}|^2) \right] \\ & - \frac{2Ea}{\Delta M^2} \left[U_{\alpha 1} U_{\alpha 2}^* (U_{\beta 1}^* U_{\beta 3} U_{e2} U_{e3}^* + U_{\beta 2} U_{\beta 3}^* U_{e1}^* U_{e3}) + U_{\beta 1}^* U_{\beta 2} (U_{\alpha 1} U_{\alpha 3}^* U_{e2} U_{e3} + U_{\alpha 2}^* U_{\alpha 3} U_{e1} U_{e3}^*) \right]. \quad (38) \end{aligned}$$

In these equations we have dropped the terms further down by $\frac{\Delta m^2}{\Delta M^2}$. Notice that the terms containing Δm^2 cancel out in $\sum_{i=1,2} (UUU\delta V)_{\alpha\beta;i3}$. Note also that only the mixing matrix elements $U_{\alpha 3}$ appear in (37) as it occurs in the oscillation probability in vacuum.

Combining all these together we obtain the expression of ΔP which is valid to first order in a :

$$\Delta P(\nu_\beta \rightarrow \nu_\alpha) \equiv P(\nu_\beta \rightarrow \nu_\alpha) - P(\bar{\nu}_\beta \rightarrow \bar{\nu}_\alpha)$$

$$\begin{aligned}
&= -4J \cos \left[\left(|U_{e1}|^2 - |U_{e2}|^2 \right) \int_0^L dx a(x) \right] \sin \left(\frac{\Delta m^2}{2E} L \right) \\
&+ 4 \text{Re}(U_{\alpha 1} U_{\alpha 2}^* U_{\beta 1}^* U_{\beta 2}) \sin \left[\left(|U_{e1}|^2 - |U_{e2}|^2 \right) \int_0^L dx a(x) \right] \sin \left(\frac{\Delta m^2}{2E} L \right) \\
&+ \frac{16Ea}{\Delta m^2} \text{Re} \left[U_{\alpha 1} U_{\alpha 2}^* U_{e1}^* U_{e2} \left(|U_{\beta 2}|^2 - |U_{\beta 1}|^2 \right) \right. \\
&+ \left. U_{\beta 1}^* U_{\beta 2} U_{e1} U_{e2}^* \left(|U_{\alpha 2}|^2 - |U_{\alpha 1}|^2 \right) \right] \sin^2 \left(\frac{\Delta m^2}{4E} L \right) \\
&+ \frac{16Ea}{\Delta M^2} \text{Re} \left[U_{\alpha 1} U_{\alpha 2}^* (U_{\beta 1}^* U_{\beta 3} U_{e2} U_{e3}^* + U_{\beta 2} U_{\beta 3}^* U_{e1} U_{e3}) \right. \\
&+ \left. U_{\beta 1}^* U_{\beta 2} (U_{\alpha 1} U_{\alpha 3}^* U_{e2} U_{e3} + U_{\alpha 2}^* U_{\alpha 3} U_{e1} U_{e3}^*) \right] \sin^2 \left(\frac{\Delta m^2}{4E} L \right) \\
&- \frac{32Ea}{\Delta M^2} |U_{e3}|^2 \left[2|U_{\alpha 3}|^2 |U_{\beta 3}|^2 - \left(\delta_{\alpha e} |U_{\beta 3}|^2 + \delta_{\beta e} |U_{\alpha 3}|^2 \right) \right] \sin^2 \left(\frac{\Delta M^2}{4E} L \right) \tag{39}
\end{aligned}$$

where the term proportional to $\text{Im}(UUU\delta V)$ and the a -dependent piece in the last term in (39) are ignored because it is of order a^2 or higher.

A few remarks are in order concerning the sign of ΔM^2 and Δm^2 . Strictly speaking, the matter effect distinguishes between the neutrino mass spectra of the types (A-1) and (A-2), or (B-1) and (B-2) defined in Fig. 2. However, with our choice of mass hierarchy, $\Delta P(\nu_\beta \rightarrow \nu_\alpha)$ barely depends on ΔM^2 , and consequently the final results do not depend on the sign of ΔM^2 . It is because the last two terms in (39) can be safely neglected due to the hierarchy in energy scales,

$$\frac{Ea}{\Delta M^2} = 1.04 \times 10^{-4} \left(\frac{\rho}{2.72 \text{gcm}^{-3}} \right) \left(\frac{E}{1 \text{GeV}} \right) \left(\frac{\Delta M^2}{1 \text{eV}^2} \right)^{-1}. \tag{40}$$

Hence, we do not distinguish between the mass patterns (A-1) and (A-2), or (B-1) and (B-2) in this work. (Note, however, that they can be distinguished by consideration of r -process nucleosynthesis in supernova [27].) For the smaller mass difference, $\Delta m^2 \equiv m_2^2 - m_1^2$, we assume that it is positive. But, it is easy to accommodate the case with negative Δm^2 in our analysis after ignoring the last two terms in (39), which we will do in our subsequent analysis. All we have to do is to change the over-all sign of $\Delta P(\nu_\beta \rightarrow \nu_\alpha)$.

By using the explicit form of the mixing matrix (5) it is then straightforward to obtain ΔP , the neutrino-antineutrino difference between oscillation probabilities, for $\nu_\mu \rightarrow \nu_e$ and $\nu_\mu \rightarrow \nu_\tau$ channels:

$$\begin{aligned}
\Delta P(\nu_\mu \rightarrow \nu_e) &\equiv P(\nu_\mu \rightarrow \nu_e) - P(\bar{\nu}_\mu \rightarrow \bar{\nu}_e) \\
&= -4J \cos \left[c_{13}^2 \cos 2\theta_{12} \int_0^L dx a(x) \right] \sin \left(\frac{\Delta m^2 L}{2E} \right) \\
&+ \left[-\sin^2 2\theta_{12} c_{13}^2 (c_{23}^2 - s_{23}^2 s_{13}^2) - 4 \cos 2\theta_{12} J \cot \delta \right] \sin \left[c_{13}^2 \cos 2\theta_{12} \int_0^L dx a(x) \right] \sin \left(\frac{\Delta m^2 L}{2E} \right) \\
&+ 4 \frac{Ea}{\Delta m^2} c_{13}^2 \left[\sin 2\theta_{12} \sin 4\theta_{12} c_{13}^2 (c_{23}^2 - s_{23}^2 s_{13}^2) + 4 \cos 4\theta_{12} J \cot \delta \right] \sin^2 \left(\frac{\Delta m^2 L}{4E} \right) \quad (41)
\end{aligned}$$

$$\begin{aligned}
\Delta P(\nu_\mu \rightarrow \nu_\tau) &\equiv P(\nu_\mu \rightarrow \nu_\tau) - P(\bar{\nu}_\mu \rightarrow \bar{\nu}_\tau) \\
&= 4J \cos \left[c_{13}^2 \cos 2\theta_{12} \int_0^L dx a(x) \right] \sin \left(\frac{\Delta m^2 L}{2E} \right) \\
&+ \left[\left\{ \left(\frac{1+s_{13}^2}{2} \right) \cos 2\theta_{12} \cos 2\theta_{23} - 4c_{13}^{-2} J \cot \delta \right\}^2 \right. \\
&+ \frac{1}{4} c_{13}^4 (\sin^2 2\theta_{12} + \sin^2 2\theta_{23}) - \left. \left(\frac{1+s_{13}^2}{2} \right)^2 \right] \sin \left[c_{13}^2 \cos 2\theta_{12} \int_0^L dx a(x) \right] \sin \left(\frac{\Delta m^2 L}{2E} \right) \\
&- 4 \frac{Ea}{\Delta m^2} \left[\sin 2\theta_{12} c_{13}^2 \left\{ \sin 4\theta_{12} \sin^2 2\theta_{23} \left(\frac{1+s_{13}^2}{2} \right)^2 - \sin 4\theta_{12} s_{13}^2 \right\} \right. \\
&- \left. 4 \cos 4\theta_{12} \cos 2\theta_{23} \left(\frac{1+s_{13}^2}{2} \right) J \cot \delta + 32 \cos 2\theta_{12} c_{13}^{-2} J^2 \cot^2 \delta \right] \sin^2 \left(\frac{\Delta m^2 L}{4E} \right) \quad (42)
\end{aligned}$$

For completeness we also give the expression of ΔP for $\nu_e \rightarrow \nu_\tau$ channel:

$$\begin{aligned}
\Delta P(\nu_e \rightarrow \nu_\tau) &\equiv P(\nu_e \rightarrow \nu_\tau) - P(\bar{\nu}_e \rightarrow \bar{\nu}_\tau) \\
&= -4J \cos \left[c_{13}^2 \cos 2\theta_{12} \int_0^L dx a(x) \right] \sin \left(\frac{\Delta m^2 L}{2E} \right) \\
&+ \left[-\sin^2 2\theta_{12} c_{13}^2 (s_{23}^2 - c_{23}^2 s_{13}^2) + 4 \cos 2\theta_{12} J \cot \delta \right] \sin \left[c_{13}^2 \cos 2\theta_{12} \int_0^L dx a(x) \right] \sin \left(\frac{\Delta m^2 L}{2E} \right) \\
&+ 4 \frac{Ea}{\Delta m^2} c_{13}^2 \left[\sin 2\theta_{12} \sin 4\theta_{12} c_{13}^2 (s_{23}^2 - c_{23}^2 s_{13}^2) - 4 \cos 4\theta_{12} J \cot \delta \right] \sin^2 \left(\frac{\Delta m^2 L}{4E} \right) \quad (43)
\end{aligned}$$

Let us compare these analytic results with the exact solutions obtained in [28] for a constant matter density to examine the accuracy of our approximate formulas. We pick up the following two parameter sets,

$$(a) \quad s_{23}^2 = 3.0 \times 10^{-3}, s_{13}^2 = 2.0 \times 10^{-2} \quad (44)$$

$$(b) \quad s_{23}^2 = 2.0 \times 10^{-2}, s_{13}^2 = 0.98 \quad (45)$$

from the allowed regions (A) and (B), respectively. These parameters are chosen so that J takes a maximal value within the each allowed region and are plotted in Fig. 1. We will use the same parameter sets also in our analyses in the following sections. To obtain the “exact

results” by using the analytic expressions given in [28] we take an average over the rapid oscillations due to the larger mass difference ΔM^2 . We take the constant matter density and electron fraction, $\rho = 2.72 \text{ g/cm}^3$ and $Y_e = 0.5$. In Fig. 3 we show the comparison between the exact and approximated values of $\Delta P(\nu_\mu \rightarrow \nu_e)$ and $\Delta P(\nu_\mu \rightarrow \nu_\tau)$. We have fixed the remaining parameters as $s_{12}^2 = 0.3$, $\Delta M^2 = 5 \text{ eV}^2$ and $\delta = \pi/2$. We see that for $E \sim 1 \text{ GeV}$ the approximation is very good even for smaller values of Δm^2 ($\sim 10^{-3} \text{ eV}^2$) than the one we assumed in eq. (7).

VI. CP VIOLATION VS. MATTER EFFECT IN LONG-BASELINE NEUTRINO OSCILLATION EXPERIMENTS: AN ORDER-OF-MAGNITUDE ANALYSIS

In this section we present the results of our order estimations of the magnitude of CP violation, and give an answer to the question of relative importance between the genuine CP -violating and the matter effects. This precedes the presentation of the results of detailed numerical computation in the next section, which will provide us complementary informations. The order-of-magnitude estimation based on our analytic expressions of ΔP illuminates the general features of the interplay between the CP phase and the matter effects, and is valid in whole allowed parameter regions. On the other hand, the numerical computation using the exact expression of the oscillation probability (albeit under the constant density ansatz) will reveal precise features of the relative importance between competing two effects.

For convenience of our discussion let us denote the three terms in (41) and (42) as

$$\begin{aligned} \Delta P(\nu_\beta \rightarrow \nu_\alpha) &= \Delta P_{\beta\alpha}^{CP} + \Delta P_{\beta\alpha}^{matter1} + \Delta P_{\beta\alpha}^{matter2} \\ &\equiv C_{\beta\alpha}^{CP} \sin \Delta + C_{\beta\alpha}^{matter1} \sin \Delta + C_{\beta\alpha}^{matter2} \sin^2(\Delta/2), \quad (\beta = \mu, \alpha = e, \tau), \end{aligned} \quad (46)$$

where $\Delta \equiv \Delta m^2 L/2E$, which can be of order 1 for $\Delta m^2 \lesssim 10^{-2} \text{ eV}^2$, $E \gtrsim 1 \text{ GeV}$ and $L \gtrsim 100 \text{ km}$. $C_{\beta\alpha}^{CP}$ is the coefficient of the first term in these equations which represents the genuine CP violating effect corrected by the matter effect. $C_{\beta\alpha}^{matter1}$ and $C_{\beta\alpha}^{matter2}$ are the coefficients in the second and third terms in (41) and (42), display the matter effects

from the different sources. That is, $C_{\beta\alpha}^{matter1}$ represents the matter effect which arises due to the evolution of the phase of the neutrino wave function in matter, whereas $C_{\beta\alpha}^{matter2}$ comes from the correction to the mixing matrix, as exhibited in the $UUU\delta V$ factors in (33). We notice that $C_{\beta\alpha}^{CP}$ and $C_{\beta\alpha}^{matter1}$ contain the integral $\int_0^L dx a(x)$ which can be estimated, by assuming the constant density 2.72 g/cm^3 , as $aL = 1.2 \times 10^{-1}$ for KEK-PS→Super-Kamiokande experiment with baseline of 250 km, and $aL = 3.5 \times 10^{-1}$ for MINOS or CERN-ICARUS experiment with baseline of 730 km or 732 km, respectively. On the other hand, $C_{\beta\alpha}^{matter2}$ carries the coefficient $Ea/\Delta m^2$ which is of the order of $\sim 10^{-2}$ for $E \sim 1 \text{ GeV}$ and $\Delta m^2 \sim 10^{-2} \text{ eV}^2$. Therefore, apart from prefactors which depend on mixing angles, we estimate that

$$C_{\beta\alpha}^{CP} \propto -4J \sim 10^{-2}, \quad (47)$$

$$C_{\beta\alpha}^{matter1} \propto aL \sim 0.1, \quad (48)$$

$$C_{\beta\alpha}^{matter2} \propto \frac{2Ea}{\Delta m^2} \sim 10^{-2}. \quad (49)$$

We recognize that $C_{\beta\alpha}^{matter1}$ can be much larger, depending on the mixing angles, than the genuine CP violating effect $C_{\beta\alpha}^{CP}$. We also note that from eq. (49) it is clear that if we assume smaller Δm^2 values $C_{\beta\alpha}^{matter2}$ become larger (See also the Tables 1 and 2).

In Table 1 we summarize the results of our order-of-magnitude estimation of these three coefficients for $\nu_\mu \rightarrow \nu_e$ channel. In doing the estimation we have taken into account the coefficient which depend on the mixing angles, and the numbers presented in Table 1 refers to the possible maximal values in each region. We notice that, if $\sin \Delta \sim 1$, in the region (A) the oscillation probability $P(\nu_\mu \rightarrow \nu_e)$ can be large, ~ 1 , but CP violation due to the matter effect is much larger than the intrinsic CP violation effect, $\Delta P^{CP} \sim 0.1 \times \Delta P^{matter}$. On the other hand, in the region (B), $P(\nu_\mu \rightarrow \nu_e)$ is small, $\sim 10^{-2}$, but the contamination of matter effect in CP violation is very small, $\Delta P^{matter} \sim 10^{-4}$ compared to $\Delta P^{CP} \sim 10^{-2}$.

In Table 2, we present the same quantities for $\nu_\mu \rightarrow \nu_\tau$ channel. We observe that in this channel the intrinsic CP violating effect is larger than the matter effect in both regions (A) and (B), i.e., $\Delta P^{CP} \sim 10^{-2}$ whereas $\Delta P^{matter} \sim 10^{-3}$.

Let us try to understand the qualitative features of these results. Probably, the most interesting aspect of our results is that the matter effect is small in the region (B) in $\nu_\mu \rightarrow \nu_e$ channel. But, in fact it is not difficult to understand the reason why. In the region (B) the mixing parameters are such that ν_e is much heavier than ν_μ and ν_τ , which are almost degenerate, or that ν_μ and ν_τ are heavier than ν_e by the same amount in the mass hierarchies given in Fig. 2. The matter effect only affects electron neutrinos and the matter potential is small compared with ν_e - ν_μ mass difference, $\Delta M^2/E \gg a$. Then, it is easy to expect that the matter effect is small not only in $\nu_\mu \rightarrow \nu_\tau$ but also in $\nu_\mu \rightarrow \nu_e$ channels.

In the region (A), on the other hand, ν_τ is much heavier than ν_e and ν_μ , or vice versa, and ν_e and ν_μ are strongly mixed. Therefore, one would naively expect that the matter effect is sizable, as it is indeed the case in $\nu_\mu \rightarrow \nu_e$ channel. But, the situation is different in $\nu_\mu \rightarrow \nu_\tau$ channel. A ν_μ can easily communicate with ν_e and thus feels the effect of earth matter but to make oscillation into ν_τ it has to overcome the huge mass difference compared with the matter potential. Therefore, the matter effect is not dominant in the region (A) of $\nu_\mu \rightarrow \nu_\tau$ channel.

VII. CP VIOLATION VS. MATTER EFFECT IN LONG-BASELINE NEUTRINO OSCILLATION EXPERIMENTS: A NUMERICAL ANALYSIS

In this section we present the results of our numerical analysis using the two sets of parameters (a) and (b) given in (45) and (45). We do this first for $\nu_\mu \rightarrow \nu_e$ channel, and second for $\nu_\mu \rightarrow \nu_\tau$ channel. All the calculations are carried out by using the exact analytic expressions found in [28] with the procedure mentioned at the end of section V.

A. $\nu_\mu \rightarrow \nu_e$ and $\bar{\nu}_\mu \rightarrow \bar{\nu}_e$ channels

First let us take the parameter set (a). In Fig. 4 we plot $P(\nu_\mu \rightarrow \nu_e)$ and $P(\bar{\nu}_\mu \rightarrow \bar{\nu}_e)$ and the corresponding $\Delta P(\nu_\mu \rightarrow \nu_e) \times 100$ as a function of $\Delta m^2/E$ for different values of s_{12}^2 . We fix the distance $L = 250$ and 730 km in Figs. 4(a) and 4(b), respectively. We see that

from (iv) and (vi) in Fig. 4 that $\Delta P(\nu_\mu \rightarrow \nu_e)$ can be as large as $\sim 10\%$ for $L = 250$ km and $\sim 25\%$ for $L = 730$ km due to the matter effect whereas the intrinsic CP violation is at most $\sim 1.5\%$, in agreement with our estimation in the previous section (see Table 1). We can conclude that the matter effect dominates over genuine CP violating effect except at the exceptional point $s_{12}^2 \simeq 0.5$. As we can see from the second term in eq. (41) that the matter potential is multiplied by $\cos 2\theta_{12}$ and hence the matter effect in $\Delta P(\nu_\mu \rightarrow \nu_e)$ is suppressed if s_{12}^2 is close to 0.5. This suppression can also be seen in Fig. 3 in the first reference in [13]. We also notice that this factor $\cos 2\theta_{12}$ gives rise to the sign difference in $\Delta P(\nu_\mu \rightarrow \nu_e)$ for $s_{12}^2 > 0.5$ and $s_{12}^2 < 0.5$ as we can confirm from (iv) and (vi) in Fig. 4.

In Fig. 5 we plot the contour of $\Delta P(\nu_\mu \rightarrow \nu_e)$ on the $s_{12}^2 - \Delta m^2/E$ plane to see the global features of the coexisting CP and the matter effects. We see that the contours for the pure CP and the pure matter cases are very different and the amplitude of the latter is larger. It may be difficult to see the genuine CP violating effect just by observing $\Delta P(\nu_\mu \rightarrow \nu_e)$ apart from the exceptional region $s_{12}^2 \simeq 0.5$.

Let us turn to the parameter set (b). In Fig. 6 we plot as in Fig. 4 $P(\nu_\mu \rightarrow \nu_e)$ (and for $\bar{\nu}$) and $\Delta P(\nu_\mu \rightarrow \nu_e)$ but for the parameter set (b). In this case the probabilities of $\nu_\mu \rightarrow \nu_e$ and $\bar{\nu}_\mu \rightarrow \bar{\nu}_e$ are small, of the order of 1% , as we can see in Fig. 6 and they may be denoted as the minor channels. In this case the matter effect contamination in ΔP is negligibly small, in agreement with our estimation done in the previous section. We confirm that the genuine CP violating effect dominates over the matter effect at the parameter (b).

B. $\nu_\mu \rightarrow \nu_\tau$ and $\bar{\nu}_\mu \rightarrow \bar{\nu}_\tau$ channels

In Fig. 7 we plot P and ΔP as in Fig. 4 but for the parameter set (a) in the $\nu_\mu \rightarrow \nu_\tau$ and $\bar{\nu}_\mu \rightarrow \bar{\nu}_\tau$ channels. These channels are also minor since $P \lesssim 2\%$ but $\Delta P_{\mu\tau}$ is relatively large $\sim 1\%$. We see that the genuine CP violating effect is larger than the matter effect. In Fig. 8 we plot as in Fig. 5 the contour of $\Delta P(\nu_\mu \rightarrow \nu_\tau)$ on the $s_{12}^2 - \Delta m^2/E$ plane. We confirm from these contours that the genuine CP effect is larger than the matter effect, in

agreement with our estimation given in Table 2.

In Fig. 9 we plot P and ΔP for the parameter set (b). In this case $\nu_\mu \rightarrow \nu_\tau$ is the dominant channel but ΔP is small $\sim 0.7\%$. We see that apart from the small s_{12}^2 region for the baseline $L = 730$ km the genuine CP violating effect is larger than the matter effect. Hence, we conclude that for $\nu_\mu \rightarrow \nu_\tau$ and $\bar{\nu}_\mu \rightarrow \bar{\nu}_\tau$ channels are relatively free from the matter effect. In Fig. 10 we plot the contour of $\Delta P(\nu_\mu \rightarrow \nu_\tau)$ for this parameter set. We see that also for this case the genuine CP effect is larger than the matter effect in agreement with our prediction (see Table 2).

VIII. CONCLUSION

We have investigated in detail the CP violation in long-baseline neutrino oscillation experiments in the presence of matter effect under the assumption of neutrino mass hierarchy, $\Delta m^2 \sim 10^{-2} \text{ eV}^2$ and $\Delta M^2 \sim \text{a few eV}^2$, motivated by the atmospheric neutrino anomaly and the cosmological dark matter. We developed the matter perturbation theory using the hierarchy in energy scales, $a \ll \frac{\Delta m^2}{2E}$, and derived the approximate analytic expressions of $\nu - \bar{\nu}$ difference in oscillation probabilities $\Delta P(\nu_\beta \rightarrow \nu_\alpha)$. We have found that in a good approximation ΔP can be expressed as a sum of three terms which represent the genuine CP violating effect and two different correction terms due to the matter effect. These analytic expressions of the ΔP are useful in understanding the global features of the competition of two effects.

We have studied the question of how large is the magnitude of CP violations due to intrinsic CP -violating phase and to the matter effect in the earth. The assumed mass hierarchy mentioned above and the interpretation of the atmospheric neutrino anomaly in terms of the neutrino oscillations allow us to restrict ourselves into the parameter regions strongly constrained by the reactor and the accelerator experiments, (A) small- s_{13} and small- s_{23} and (B) large- s_{13} and arbitrary s_{23} .

We have found the following structure (as summarized in Tables 1 and 2).

$\nu_\mu \rightarrow \nu_e$ channel: In the region (A) the matter effect contamination is much larger than the genuine CP violation effect except for the case $s_{12} \simeq 0.5$. Whereas in (B) the matter effect contamination is negligible compared with genuine CP violation. Unfortunately, the magnitude of the latter is small, ~ 0.5 %.

$\nu_\mu \rightarrow \nu_\tau$ channel: The matter contamination is smaller than the genuine CP violation effect and is not harmful in both regions (A) and (B). The magnitude of the CP violation is again not sizable, ~ 1 %.

Thus, if the mass hierarchy motivated by the dark matter is the truth in nature, it appears to be necessary to invent new method for measuring CP violation of ~ 1 % level in long-baseline neutrino oscillation experiments. We are planning to discuss an idea toward the goal elsewhere [29].

Note added: While we were to complete this paper we became aware of the paper by Arafune et al. [30] which addresses the similar topics. However, they consider different neutrino mass spectrum and employ a different approximation scheme from ours which requires that $\frac{aL}{E} \ll 1$ and $\frac{\Delta m^2 L}{E} \ll 1$, whereas we only need $\frac{Ea}{\Delta m^2} \ll 1$.

We also note that after this paper had been submitted for publication, a new data on atmospheric neutrinos from Super-Kamiokande experiment has appeared [31]. The data seem to favor smaller values of Δm^2 than the one we assumed in this paper. However, the results of the analysis done in this paper is presented so that they are useful for such smaller values of Δm^2 . We stress that the perturbative treatment of the matter effect is still valid even for Δm^2 as small as 10^{-3} eV^2 .

Acknowledgements

We thank Masafumi Koike, Joe Sato and Osamu Yasuda for pointing out an error in our earlier version of this paper and for discussions which led us to the clarification of the point. One of us (H.M.) was supported partially by Grant-in-Aid for Scientific Research on Priority Areas under #08237214 and is supported in part by Grant-in-Aid for Scientific Research

#09045036 under International Scientific Research Program, Inter-University Cooperative Research. The other (H.N.) has been supported by a DGICYT postdoctoral fellowship at Universitat de València under Grant PB95-1077 and TMR network ERBFMRXCT960090 of the European Union.

APPENDIX

We verify that the adiabatic approximation which we have employed to obtain (17) is in fact a very good approximation for the long-baseline neutrino experiments. The adiabaticity condition is nothing but the condition

$$\left| \left[\frac{d}{dx} V^+(x) \cdot V(x) \right]_{ij} \right| \ll |(H_d)_{ii}| \quad (50)$$

To first order in matter perturbation theory the off-diagonal elements of the LHS of (50) can be expressed as

$$\left[\frac{d}{dx} V^+(x) \cdot V(x) \right]_{ij} = -a'(x) \frac{U_{ej}^* U_{ei}}{h_j^{(0)} - h_i^{(0)}}$$

for $i \neq j$ and the diagonal elements vanish for $i = j$. Then the adiabaticity condition can be written as

$$|U_{ej}^* U_{ei}| \ll \left| \frac{1}{a'(x)} \right| \left(\frac{\Delta m^2}{2E} \right)^2 \quad (51)$$

where the RHS is replaced by Δm^2 , the smallest Δm_{ij}^2 . The expression (51) in fact represents the sufficient condition, but we will see that it is well satisfied.

The density gradient in the continental structure is at most 0.2g/cm^3 over the depth of 20 km [26], which amount to the baseline of 1000 km. Using this $a'(x)/a(x)$ can be estimated as

$$\left| \frac{a'(x)}{a(x)} \right| \simeq 1.5 \times 10^{-4} \text{km}^{-1}$$

Then, the the adiabaticity condition reads

$$|U_{ej}^* U_{ei}| \ll 0.83 \times 10^4 \left(\frac{\Delta m^2}{10^{-2} \text{eV}^2} \right)^2 \left(\frac{E}{1 \text{GeV}} \right)^{-2} \left(\frac{a'}{4 \times 10^{-4} \text{gcm}^{-3} \text{km}^{-1}} \right)^{-1}$$

It is clear that the adiabaticity condition is well satisfied in the long baseline experiments due to the slow variation of matter density in the continental structure.

REFERENCES

- [1] B. T. Cleveland et al., Nucl. Phys. B (Proc. Suppl.) **38**, 47 (1995); Y. Suzuki, *ibid* **38**, 54 (1995); P. Anselmann et al., Phys. Lett. **B285**, 376 (1992); **B314**, 445 (1993); **327**, 377 (1994); **B342**, 440 (1995); J. N. Abdurashitov et al., Nucl. Phys. B (Proc. Suppl.) **38**, 60 (1995).
- [2] K. S. Hirata et al., Phys. Lett. **B205**, 416 (1988); **B280**, 146 (1992); Y. Fukuda et al., *ibid* **B335**, 237 (1994); R. Becker-Szendy et al., Phys. Rev. **D46**, 3720 (1992); W. W. M. Allison et al., Phys. Lett. **B391**, 491 (1997).
- [3] N. Cabbibo, Phys. Rev. Lett. **10**, 531 (1963); M. Kobayashi and T. Maskawa, Prog. Theor. Phys. **49**, 652 (1973).
- [4] M. Fukugita and T. Yanagida, Phys. Lett. **B174**, 45 (1986).
- [5] N. Cabbibo, Phys. Lett. **B72**, 333 (1978).
- [6] V. Barger, K. Wisnant and R. J. N. Phillips, Phys. Rev. Lett. **45**, 2084 (1980).
- [7] S. Pakvasa, in *Proceedings of the XXth International Conference on High Energy Physics*, edited by L. Durand and L. G. Pondrom, AIP Conf. Proc. No. 68 (AIP, New York, 1981), Vol. 2, pp. 1164.
- [8] S. M. Bilenky, J. Hosek and S. T. Petcov, Phys. Lett. **B94**, 495 (1980).
- [9] C. Jarlskog, Phys. Rev. Lett. **55**, 1039 (1985).
- [10] K. Nishikawa et al., Proposal for a Long Baseline Neutrino Oscillation Experiment using KEK-PS and Super-Kamiokande, February 1995.
- [11] The MINOS Collaboration, MINOS Experiment R&D Plan: FY 1996-1998, June 1996.
- [12] The ICARUS Collaboration, ICARUS II, A Second-Generation Proton Decay Experiment and Neutrino Observatory at the Gran Sasso Laboratory, September 1993.

- [13] M. Tanimoto, Phys. Rev. **D55**, 322 (1997); M. Tanimoto, Prog. Theor. Phys. **97**, 901 (1997).
- [14] J. Arafune and J. Sato, Phys. Rev. **D55**, 1653 (1997).
- [15] L. Wolfenstein, Phys. Rev. **D17**, 2369 (1978).
- [16] T. K. Kuo and J. Pantaleone, Phys. Lett. **B198**, 406 (1987); P. I. Krastev and S. T. Petcov, Phys. Lett. **B205**, 84 (1988).
- [17] M. Aglietta et al., Europhys. Lett. **8(7)**, 611 (1989); K. Daum et al., Z. Phys. **C66**, 417 (1995).
- [18] J. A. Holtzman, Astrophys. J. Suppl. **71**, 1 (1989); J. A. Holtzman and J. R. Primack, Astrophys. J. **405**, 428 (1993); J. R. Primack, J. Holtzman, A. Klypin, and D. O. Caldwell, Phys. Rev. Lett. **74**, 2160 (1995); K. S. Babu, R. K. Schaefer, and Q. Shafi, Phys. Rev. **D53**, 606 (1996); D. Pogosyan and A. Starobinsky, astro-ph/9502019.
- [19] H. Minakata, Phys. Rev. **D52**, 6630 (1995); Phys. Lett. **B356**, 61 (1995); S. M. Bilenky, A. Bottino, C. Giunti, and C. W. Kim, Phys. Lett. **B356**, 273 (1995); G. L. Fogli, E. Lisi, and G. Scioscia, Phys. Rev. **D52**, 5334 (1995).
- [20] C. Athanassopoulos et al (LSND Collaboration), Phys. Rev. Lett. **77**, 3082 (1996); Phys. Rev. **C54**, 2685 (1996); Report nucl-ex/9706006. See also, J. E. Hill, Phys. Rev. Lett. **75**, 2654 (1995).
- [21] A. Acker and S. Pakvasa, Phys. Lett. **B397** 209 (1997).
- [22] D. Ayres, Talk given at 4th KEK Topical Conference on Flavor Physics, Tsukuba, Japan, October 29-31, 1996.
- [23] For a review, see e.g., M. White and D. Scott, Comments Astrophys. **18**, 289 (1966).
- [24] G. L. Fogli et al., in Ref. [19].

- [25] T. Yanagida, in Proceedings of the Workshop on Unified Theyroy and Baryon Number on the Universe, Tsukuba, Ibaraki, Japan, 1979, edited by O. Sawada and A. Sugamoto, KEK Report No. 79-18, pp 95, Tsukuba, 1979; M. Gell-Mann, P. Ramond and R. Slansky, in *Supergravity*, Proceedings of the Workshop, Stony Brook, New York, 1979, edited by P. van Nieuwenhuizen and D. Freedman, pp 315, (North-Holland, Amsterdam, 1979).
- [26] F. D. Stacey, *Physics of the Earth, second edition*, (John Willy & Sons, New York, 1977).
- [27] We note that the mass spectrum (A-1) or (B-2) in Fig. 2 could be in conflict with successful heavy elements nucleosynthesis in supernova. The resonant conversion between ν_e and ν_τ (or ν_μ) would be very adiabatic, possibly except for very small mixing angles, just above the neutrino sphere if $|\Delta M^2| \gtrsim$ a few eV^2 . On the other hand, for the spectrum (A-2) or (B-1) the conversion between $\bar{\nu}_e$ and $\bar{\nu}_\tau$ (or $\bar{\nu}_\mu$) would again be very adiabatic and the nucleosynthesis could be enhanced. See Y.-Z. Qian *et al.*, Phys. Rev. Lett. **71**, 1965 (1993); Y.-Z. Qian and G. M. Fuller, Phys. Rev. **D52**, 656 (1995).
- [28] H. W. Zaglauer and K. H. Schwarzer, Z. Phys. **C40**, 273 (1988). We note a typographical error in Eq. (50) in this paper; In the first term of the numerator in Eq. (50) c_{23}^2 should be replaced by c_{23} .
- [29] H. Minakata and H. Nunokawa, hep-ph/9706281, Phys. Lett. **B**, in press.
- [30] J. Arafune, M. Koike and J. Sato, Phys. Rev. **D56**, 3093 (1997).
- [31] Y. Totsuka, (Super-Kamiokande Collaboration), Talk given at International Symposium on Lepton-Photon Interactions at High Energies, July 28-August 1, 1997, Humburg, Germany.

Region	$P(\nu_\mu \rightarrow \nu_e)$	$C_{\mu e}^{CP}$	$C_{\mu e}^{matter1}$	$C_{\mu e}^{matter2}$
(A)	~ 1	$\sim 10^{-2}$	~ 0.1	$\sim 10^{-2}$ (0.1)
(B)	$\sim 10^{-2}$	$\sim 10^{-2}$	$\sim 10^{-4}$	$\sim 10^{-6}$ (10^{-5})

Table 1: The order of magnitude estimate of maximal values of P , C^{CP} and $C^{matter1,2}$ for $\nu_\mu \rightarrow \nu_e$ channel in the parameter region (A) and (B) for $E \sim 1$ GeV and $\Delta m^2 \sim 10^{-2}$ eV². For $C_{\mu e}^{matter2}$ we also show in the parentheses the values for the case $\Delta m^2 \sim 10^{-3}$ eV².

Region	$P(\nu_\mu \rightarrow \nu_\tau)$	$C_{\mu\tau}^{CP}$	$C_{\mu\tau}^{matter1}$	$C_{\mu\tau}^{matter2}$
(A)	$\sim 10^{-2}$	$\sim 10^{-2}$	$\sim 10^{-3}$	$\sim 10^{-4}$ (10^{-3})
(B)	~ 1	$\sim 10^{-2}$	$\sim 10^{-3}$	$\sim 10^{-4}$ (10^{-3})

Table 2: Same as Table 1 but for $\nu_\mu \rightarrow \nu_\tau$ channel.

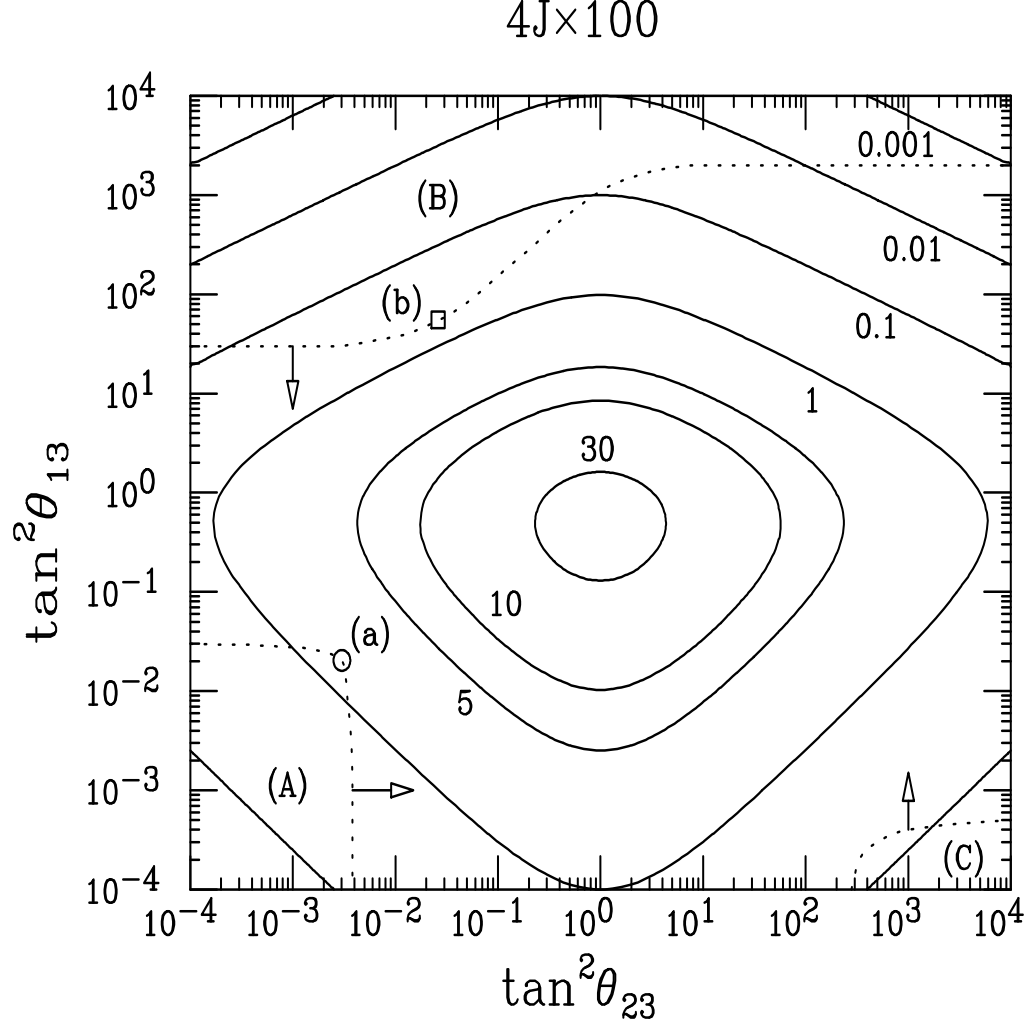


Fig. 1: Contour plot of $4J \times 100$ is shown where $J \equiv c_{12}s_{12}c_{23}s_{23}c_{13}^2s_{13}\sin\delta$. We set $\theta_{12} = \pi/4$ and $\delta = \pi/2$ which maximize J . The area indicated by dashed lines with arrows is the region excluded by accelerator and reactor experiments at 90 % C. L. obtained in ref. [24] for the case $\Delta M^2 = 5 \text{ eV}^2$. The points indicated by the (a) open circle and (b) square are the parameters we will use in this work.

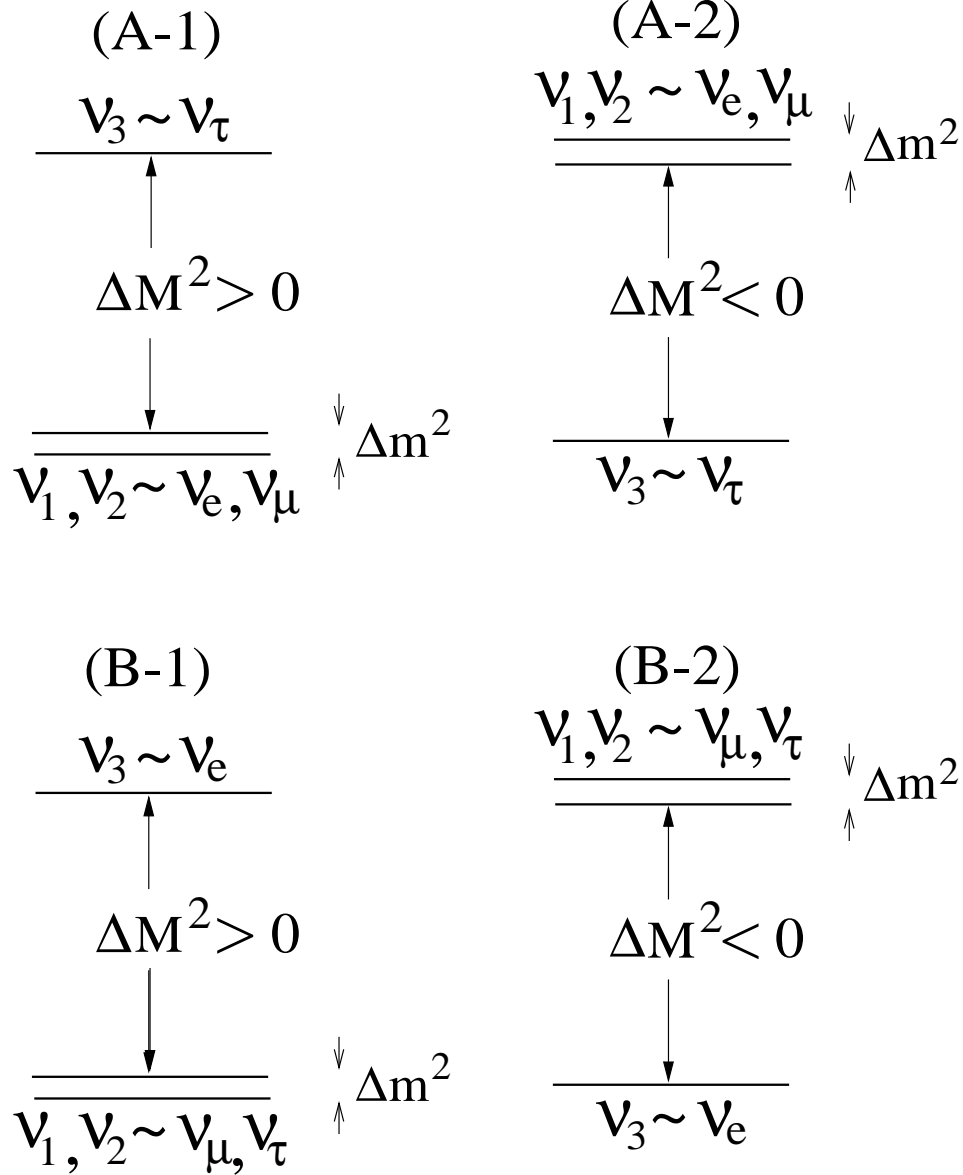


Fig. 2: The neutrino mass spectra which we consider in this paper. We assume that $\Delta M^2 \equiv m_3^2 - m_1^2 \simeq m_3^2 - m_2^2 \sim \text{a few eV}^2$ and $\Delta m^2 \equiv m_2^2 - m_1^2 \sim 10^{-2} \text{ eV}^2$. The figure (A-1,2) and (B-1,2) are for the case where mixing parameters are in the region (A) $s_{13}, s_{23} \ll 1$ and in the region (B) $s_{13} \sim 1$ and arbitrary s_{23} , respectively.

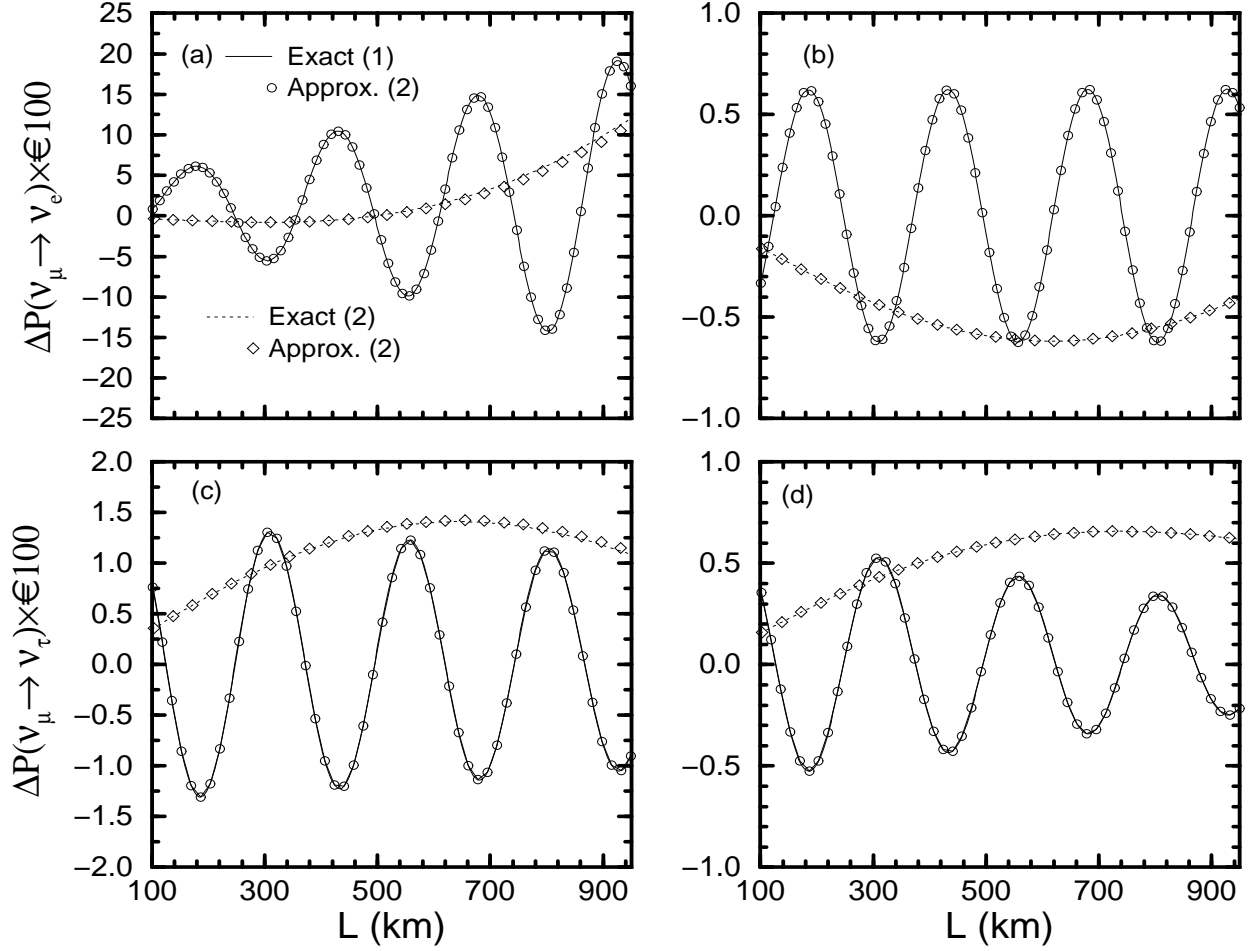


Fig. 3: We plot both the exact and approximated values of $\Delta P(\nu_\mu \rightarrow \nu_e)$ (upper two panels) and $\Delta P(\nu_\mu \rightarrow \nu_\tau)$ (lower two panels) as a function of distance L from the neutrino source. We fixed the mixing parameters as $s_{23}^2 = 3.0 \times 10^{-3}$, $s_{13}^2 = 2.0 \times 10^{-2}$ for the left two panels (a) and (c) and $s_{23}^2 = 2.0 \times 10^{-2}$, $s_{13}^2 = 0.98$ for the right two panels (b) and (d). The remaining parameters are fixed to be the same for all the case (a-d), i.e., $s_{12}^2 = 0.3$, $\Delta M^2 = 5 \text{ eV}^2$ and $\delta = \pi/2$. The solid lines and open circles are for the case $\Delta m^2/E = 10^{-2} \text{ eV}^2/\text{GeV}$ and the dotted and open diamonds are for the case $\Delta m^2/E = 10^{-3} \text{ eV}^2/\text{GeV}$.

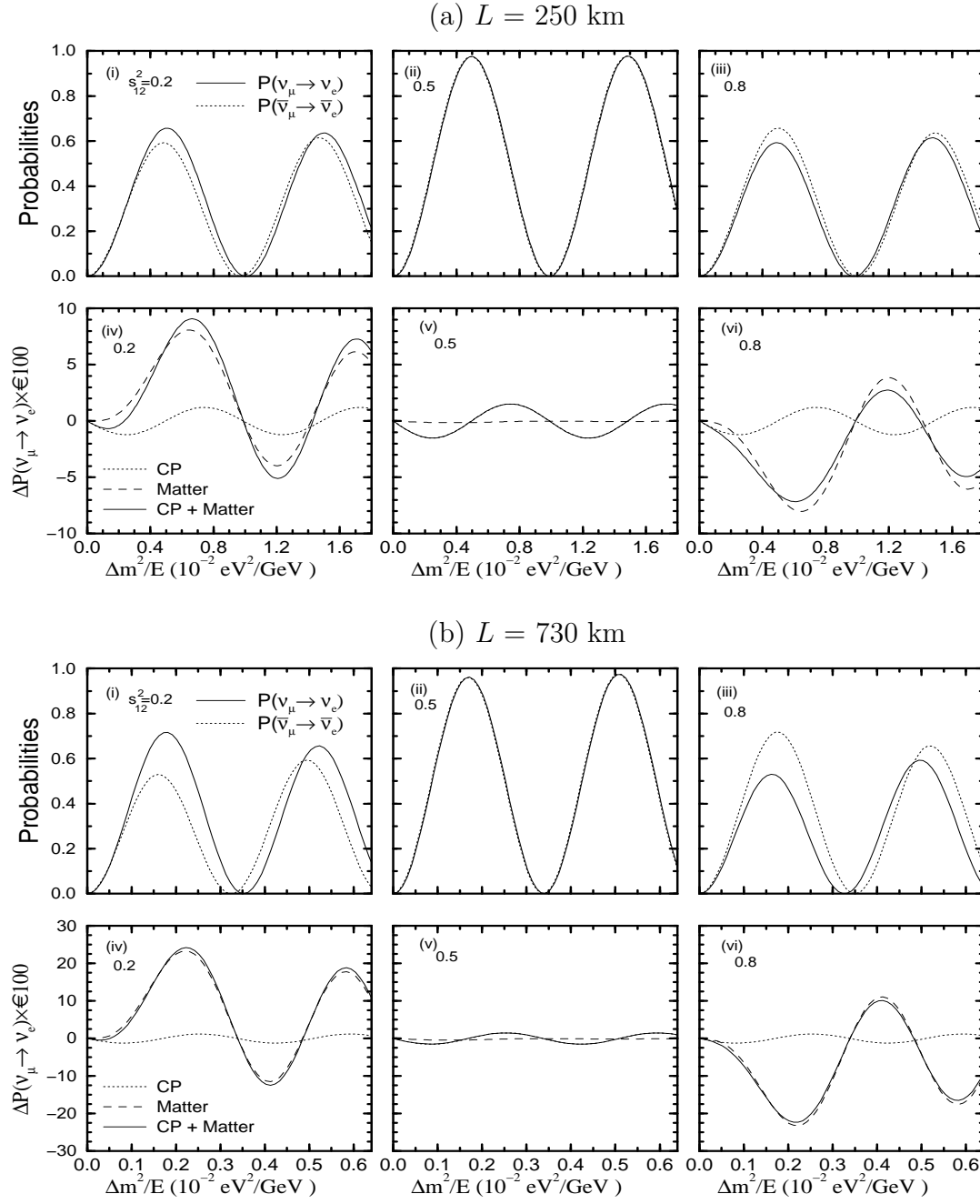


Fig. 4: We plot in (i), (ii) and (iii) $P(\nu_\mu \rightarrow \nu_e)$ and $P(\bar{\nu}_\mu \rightarrow \bar{\nu}_e)$ for the parameter set (a) $s_{23}^2 = 3.0 \times 10^{-3}$, $s_{13}^2 = 2.0 \times 10^{-2}$ as a function of $\Delta m^2/E$ for $s_{12}^2 = 0.2, 0.5$ and 0.8 , respectively. We fixed the remaining parameters as $\Delta M^2 = 5 \text{ eV}^2$, $\delta = \pi/2$. The figures (a) and (b) are for $L = 250$ km (a) and $L = 730$ km (b), respectively. In (iv), (v) and (vi) we plot the corresponding $\Delta P(\nu_\mu \rightarrow \nu_e) \times 100$ and the different curves are for the cases where only the CP (dotted line), only the matter (dashed line), and both the CP and the matter (solid line) effects are taken into account.

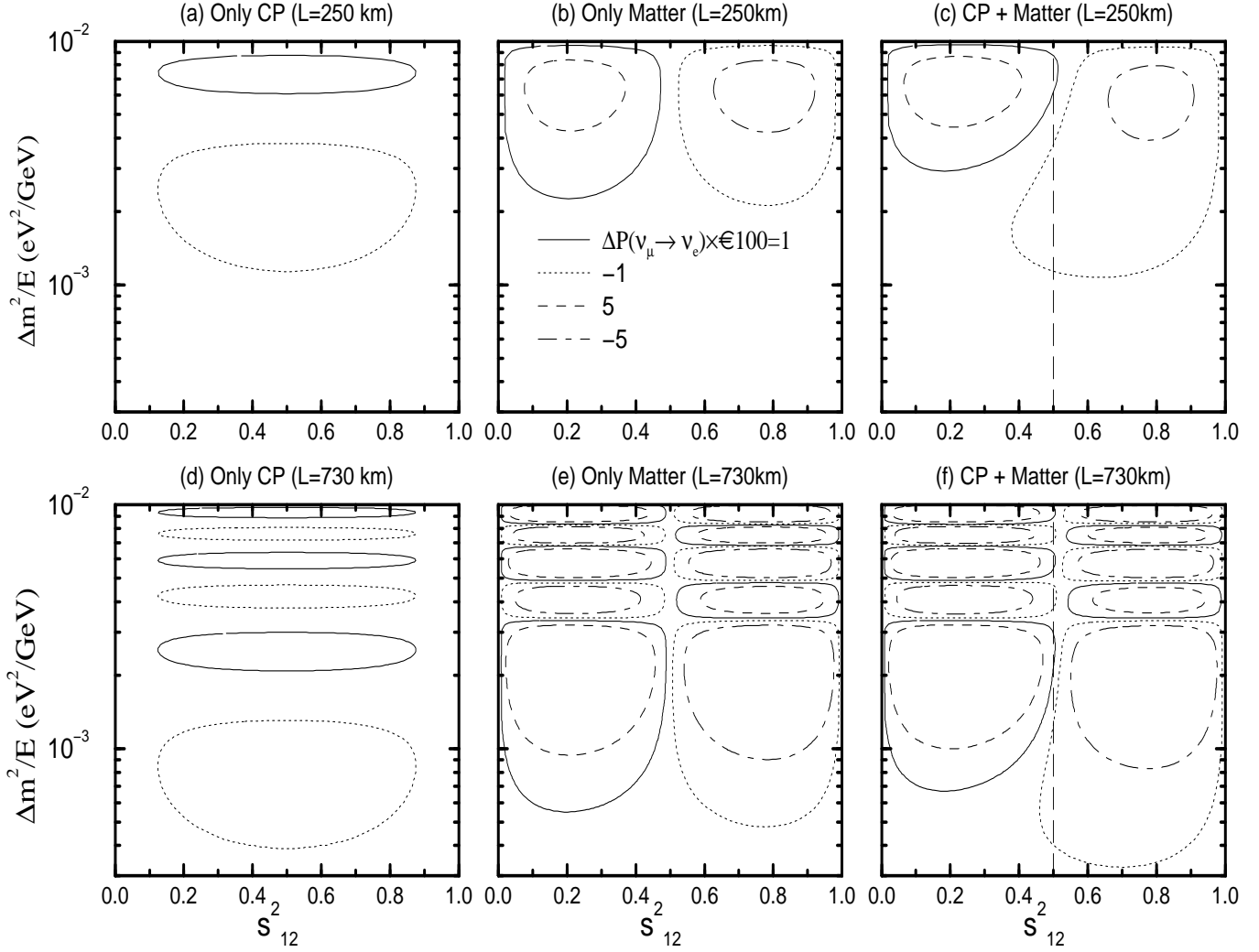


Fig. 5: We plot, for the parameter set (a) $s_{23}^2 = 3.0 \times 10^{-3}$ and $s_{13}^2 = 2.0 \times 10^{-2}$, the contour of $\Delta P(\nu_\mu \rightarrow \nu_e) \times 100$ in the $s_{12}^2 - \Delta m^2/E$ plane for the cases where only the CP effect (a, d), only the matter effect (b, e), and both the CP and the matter effects (c, f) are taken into account. The upper and the lower three panels are for $L = 250$ km and 730 km, respectively. In (c, f) we also indicate by the long-dashed symbol the line $s_{12}^2 = 0.5$ where the matter effect vanishes. The remaining parameters are fixed to be the same as in Fig. 4.

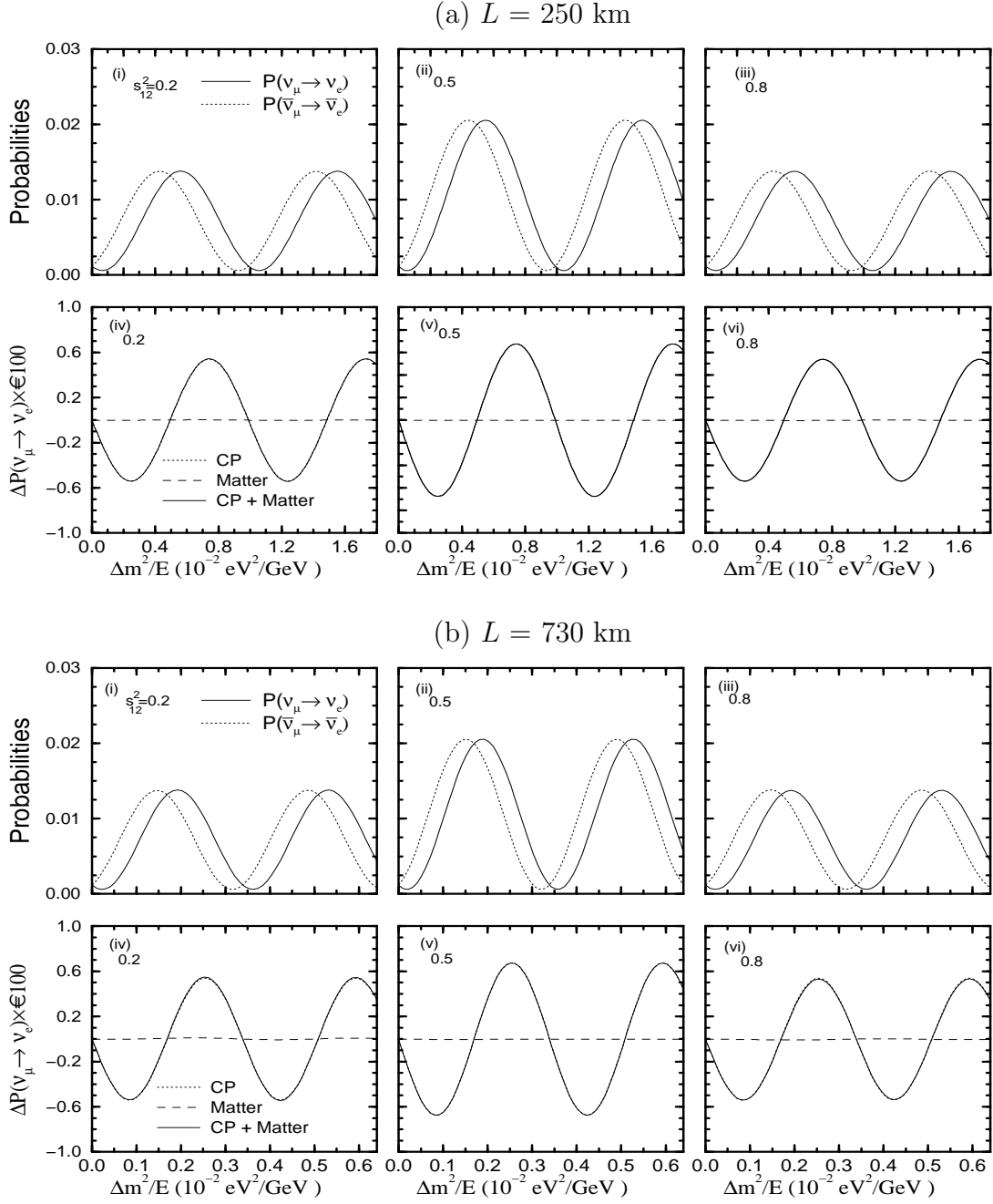


Fig. 6: Same as in Fig. 4 but for the parameter set (b) $s_{23}^2 = 2.0 \times 10^{-2}$, $s_{13}^2 = 0.98$.

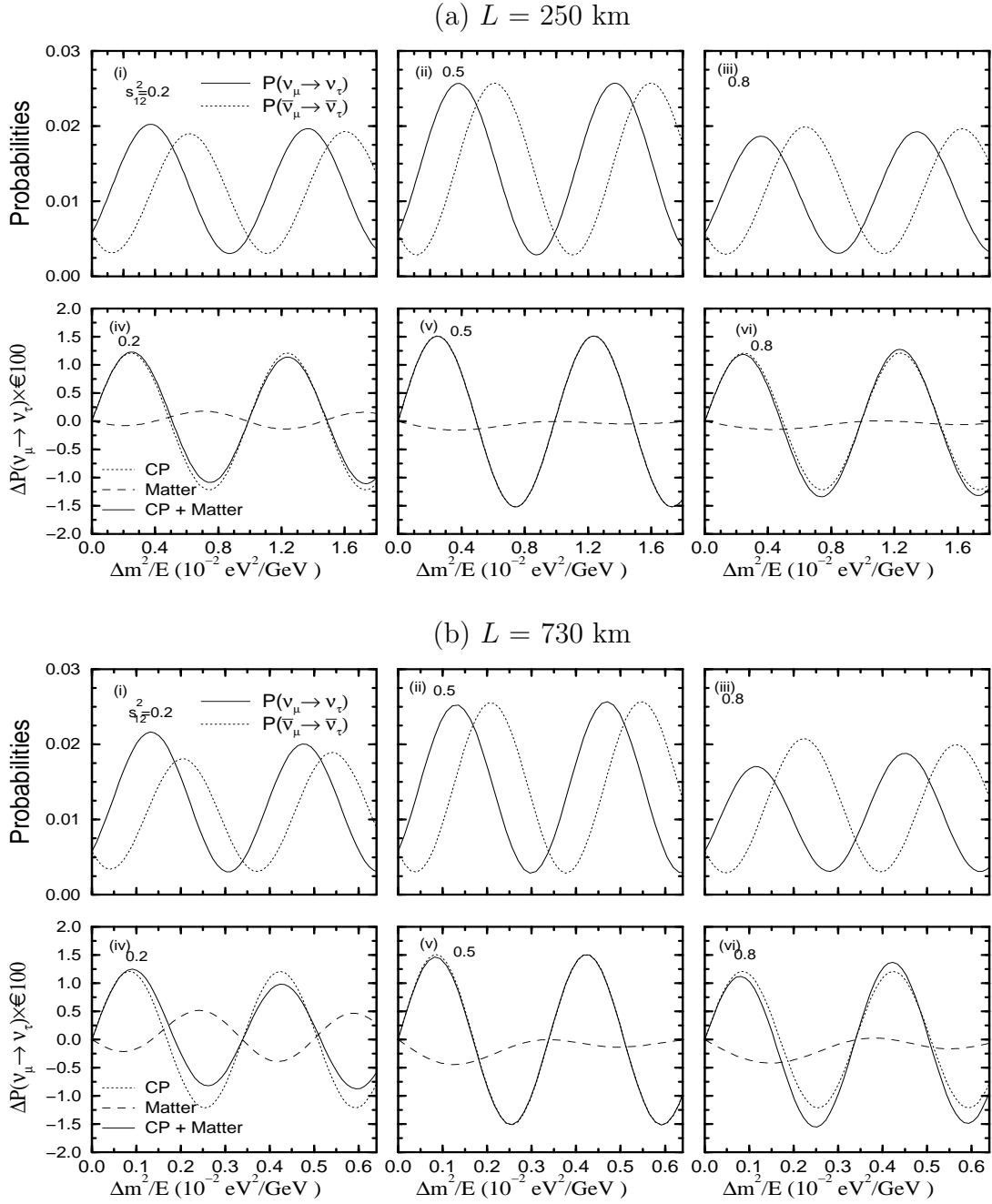


Fig. 7: Same as in Fig. 4 with the parameter set (a) $s_{23}^2 = 3.0 \times 10^{-3}$, $s_{13}^2 = 2.0 \times 10^{-2}$ but for $\nu_\mu \rightarrow \nu_\tau$ and $\bar{\nu}_\mu \rightarrow \bar{\nu}_\tau$ channels.

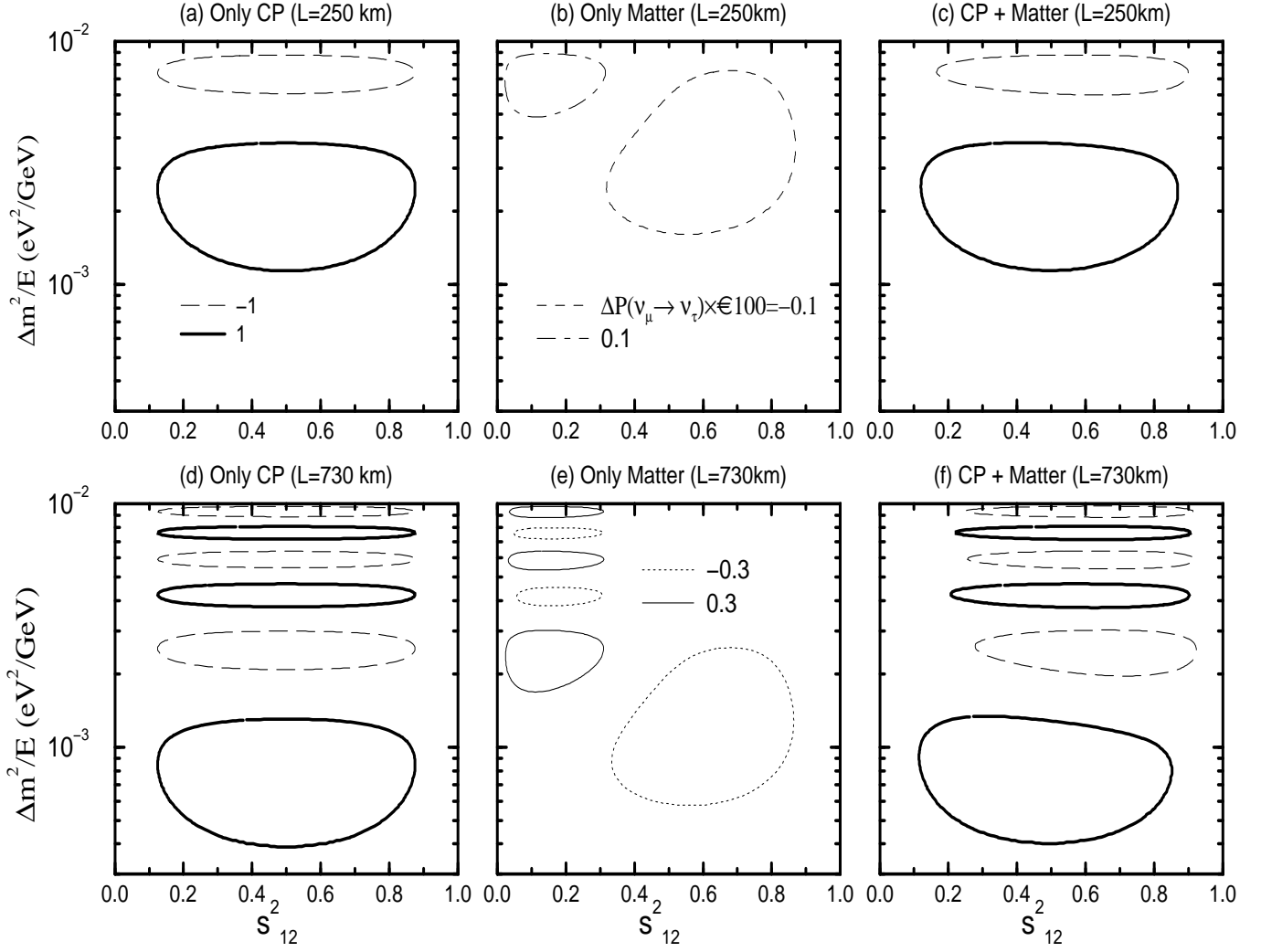


Fig. 8: Same as Fig. 5 but for $\nu_\mu \rightarrow \nu_\tau$ channel with the parameter set (a) $s_{23}^2 = 3.0 \times 10^{-3}$, $s_{13}^2 = 2.0 \times 10^{-2}$.

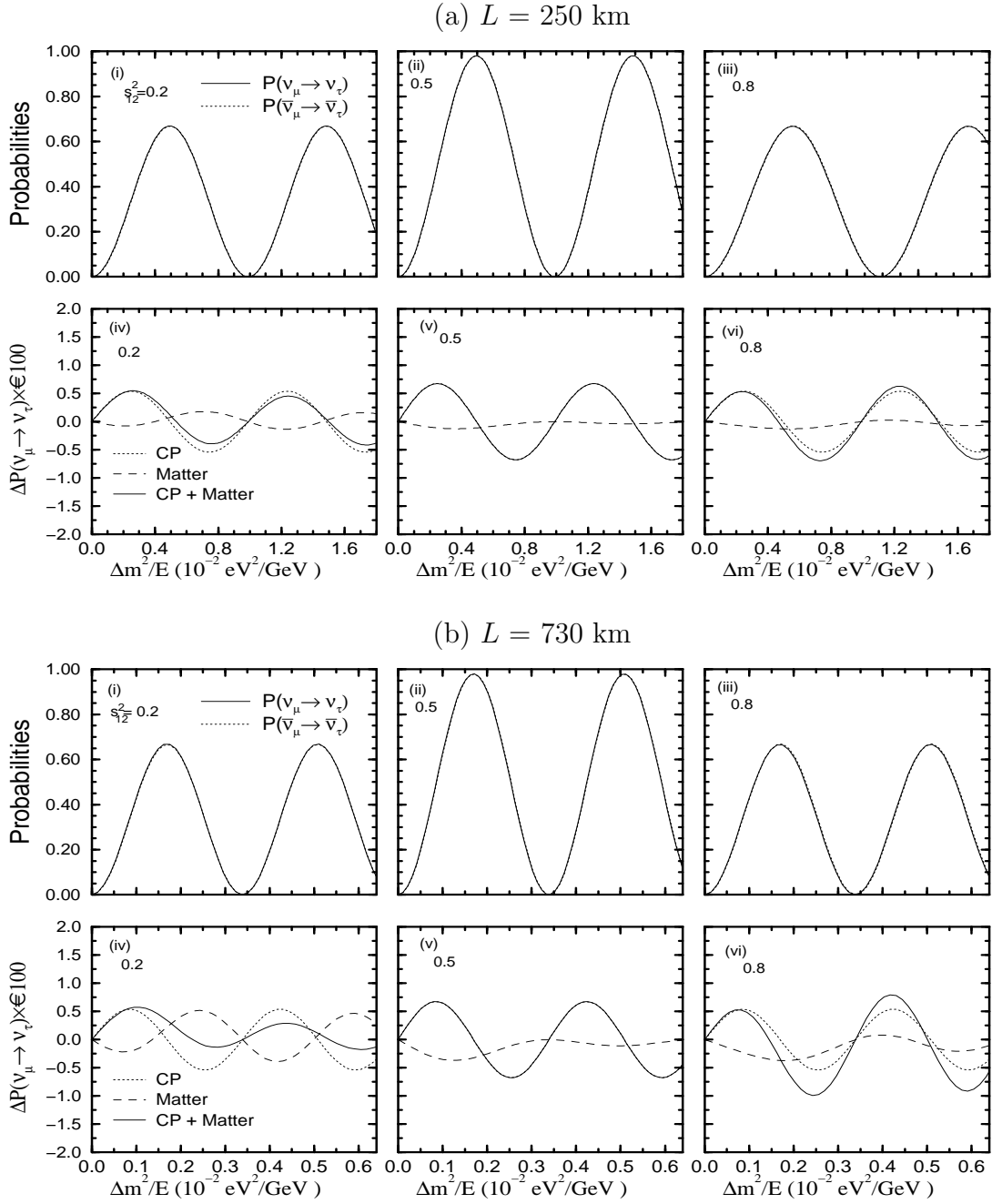


Fig. 9: Same as in Fig. 7 but for the parameter set (b) $s_{23}^2 = 2.0 \times 10^{-2}$, $s_{13}^2 = 0.98$.

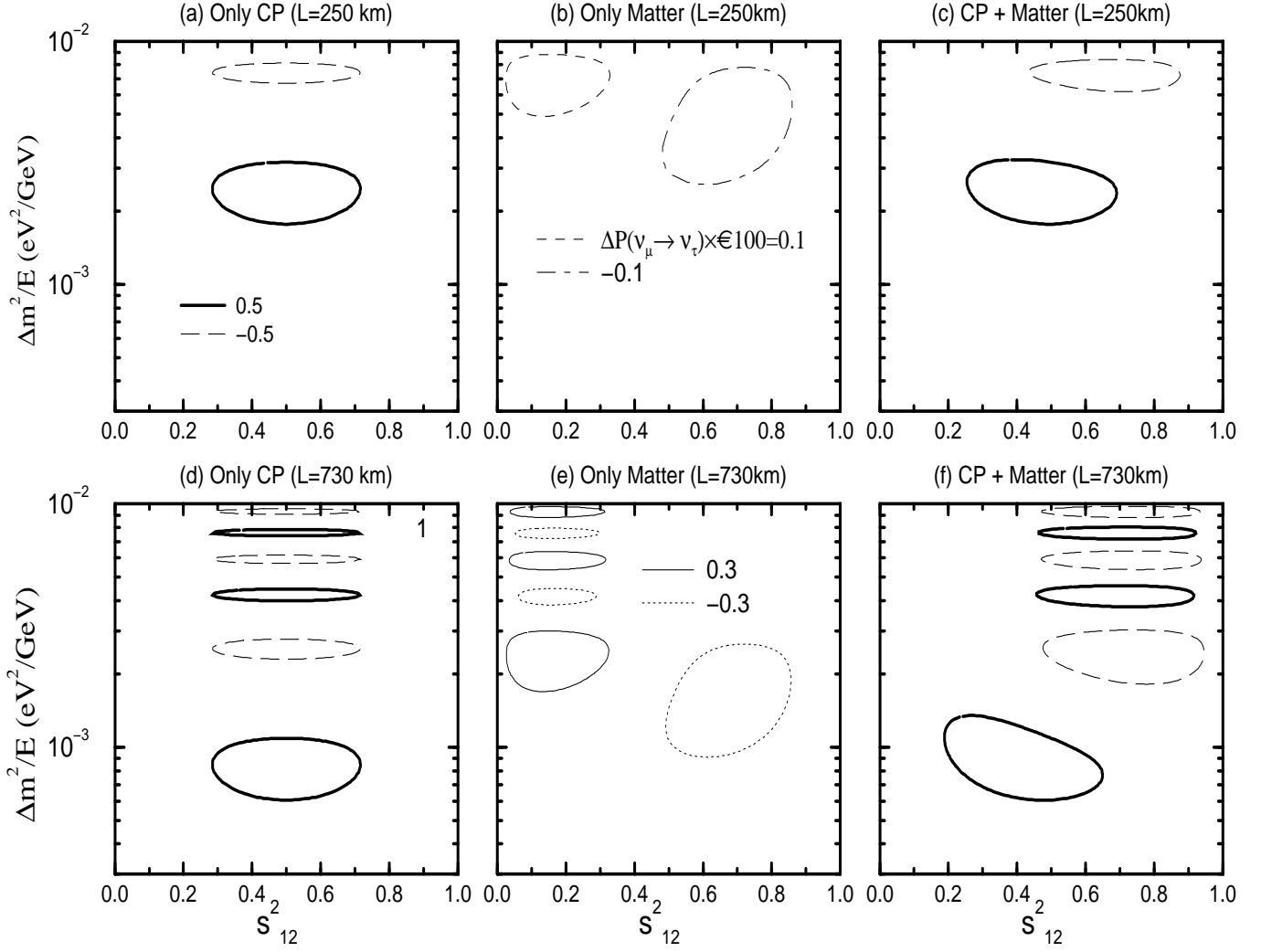


Fig. 10: Same as Fig. 8 but for the parameter set (b) $s_{23}^2 = 2.0 \times 10^{-2}$, $s_{13}^2 = 0.98$.